BEHAVIORAL ASSESSMENT OF VISION RESTORATION THROUGH OPTOGENETICS

ERIC JAMES MCDERMOTT

MASTER OF SCIENCE IN NEURAL AND BEHAVIORAL SCIENCE

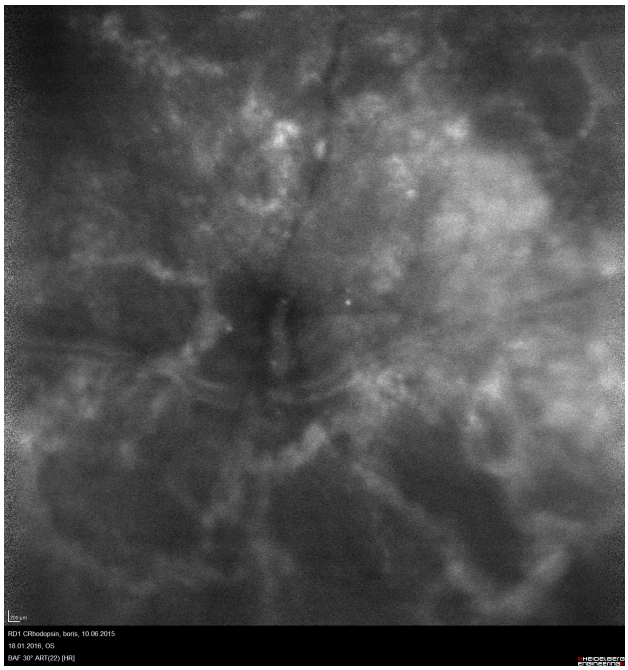

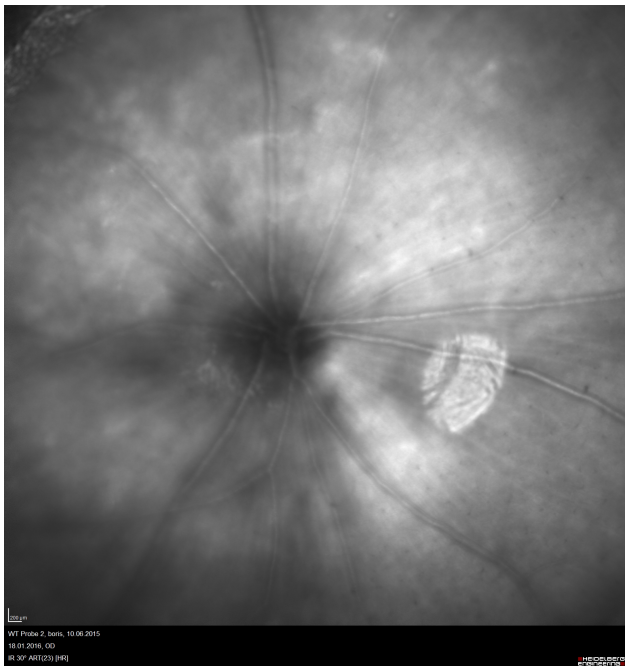

GRADUATE SCHOOL OF NEURAL & BEHAVIORAL SCIENCES
EBERHARD KARLS UNIVERSITÄT TÜBINGEN
Faculty of Science
Faculty of Medicine

Tübingen, October 2016

Eric James McDermott
Behavioral Assessment of Vision Restoration through Optogenetics
Master Thesis, October 2016
Title page figures:
OCT images of retinal degeneration and wild-type retinas [own source].

DECLARATION

Dr. Thomas Münch
Thesis Advisor
•Laboratory of Retinal Circuits and Optogenetics
•Center for Integrative Neuroscience

Prof. Dr. Jan Benda
Second Reader
•Department Head of Neuroethology
•Institute for Neurobiology

I affirm that I have written the dissertation myself and have not used any sources and aids other than those indicated.

I affirm that I have not included data generated in one of my laboratory rotations and already presented in the respective laboratory report

Eric James McDermott
Tübingen, October 2016

When you are studying any matter,
or considering any philosophy,
ask yourself only what are the facts
and what is the truth that the facts bear out.
Never let yourself be diverted either by what you wish to believe,
or by what you think would have beneficent social effects if it were believed.
But look only, and solely, at what are the facts.
Bertrand Russell

ACKNOWLEDGEMENTS

First and foremost, my parents; you have guided me through countless adventures and learning experiences while maintaining loving and nurturing hands that helped shaped this life of mine. Thank you for always believing in me, supporting me, and encouraging me.

Skip, Deirdre, Toj; thank you for always being there to listen to my crazy ideas and bounce them back in a better shape than they were in the first place.

My roommates: Jonas S., Jonas K., Coco, Tanja, Fede; thank you for all the great times, the meals together, and the general positive environment to live in and grow in throughout my time in Germany. I'll miss you all, but I know this story isn't over.

Everyone at the GTC: Barbara, Tony (you count), Yannik, Johanna, Po-hsuan, Santiago, Jonas, Ivan, Max, Nicole, Joe, Lisa, Caitlin, Seb, Nack, Judith, Theresa, Sophie, Ole, Yiling, Horst, Tina, Katja, Julia, Sandra; thank you for joining me on this journey, for the laughter, for the learning.

Jan, Juan, and the rest of the Slovenia team; thank you for showing me the beauty of researching outdoors as well as indoors, and the importance of finding that delicate balance between them. Also, I very much appreciate all the good conversations and you lending me your high-tech acoustic gear, Jan.

The lab: Marion, Saad, Boris, Elle, Thomas; thank you for being part of my day-to-day life, for showing me the ropes, and for always being there to discuss ideas and better my project. Thomas, thank you for supervising this project, constantly pushing me to better my work, and giving my idea a shot in the first place.

And lastly, myself; you did it, kid... now onto the next adventure!

ABSTRACT

Visually guided behavior is the main goal of vision. While electrophysiological, histological, and microscopic methods provide valuable insights into the functioning of the retinal circuit, there is no replacement for assessing perceptual vision through behavioral paradigms.

This thesis utilized several established and novel experimental designs in attempts to elucidate the restorative effects of two different optogenetic proteins: *Channelrhodopsin 2* and *Opto-mGluR6*. The findings suggest that although *Channelrhodopsin 2* is not ideal for clinical applications due to the extremely high (and potentially toxic) light intensity needed to elicit a visual response, *Opto-mGluR6* may indeed be a mechanism that can be used to improve visual abilities.

CONTENTS

1

BACKGROUND

Vision is one of our essential senses; a window through which we can view the world. The study of vision and visual perception dates back as far as 500 BCE with the 'emission theory' of Empedocles and ancient Greeks, who campaigned that our act of seeing represented a physical interaction with the world in which rays emanate from the eyes and intercept, even somewhat feel, objects in the world. This view was put into question by Euclid in 300BC when he asked how one could immediately perceive stars after closing and opening the eyes if one required these beams of light to travel to the objects (Wong and Kwen, 2005). Lucretius, a Roman who supported the ideas of Greek atomists, held the view in 50BC that light and heat from the sun are in the form of minute particles which shoot across the sky from their source, representing a foundation for our current understanding (Jones, Latham, and Esolen, 1996). Yet, despite the insights from Euclid and Lucretius, it is thought that the influence of Ptolemy and Galen in the 2nd century kept the 'emission theory' alive for over another thousand years. Finally, in the 18th century, Isaac Newton and John Locke, among others, asserted that light comes from objects in straight lines and enters the perceivers 'mind' through the eye. Meanwhile, Christian Huygens proposed the wave-theory of light, which was supported by the famous double-slit experiment of Thomas Young in the 19th century (Young, 1801), (Huygens, 2012). Yet, it wasn't until the early 20th century when Albert Einstein utilized the principle of quantization introduced by Max Planck that the idea of light consisting of particles, or quanta, was brought into the world (Einstein, 1965). Today, this wave/particle dual-nature of light is the scientifically held norm, and can be more thoroughly explored in a review by Richard Feynman (Feynman and Zee, 2006).

Looking past the physical nature of light and into how this light interacts with ourselves from a biological perspective, we find that after light enters the eye, a series of complex interactions with a structure known as the retina take place. The retina was first described in detail by Santiago Ramón y Cajal in 1894 (Cajal, 1960), (Cajal, 1972). Currently, the retina is described as being composed of 5-main neural cell types: Photoreceptors (Rods and Cones), Horizontal cells, Bipolar cells, Amacrine cells, and Ganglion cells (figure 1). Each of these cell types represents a step in the pathway from light sensation to light perception.

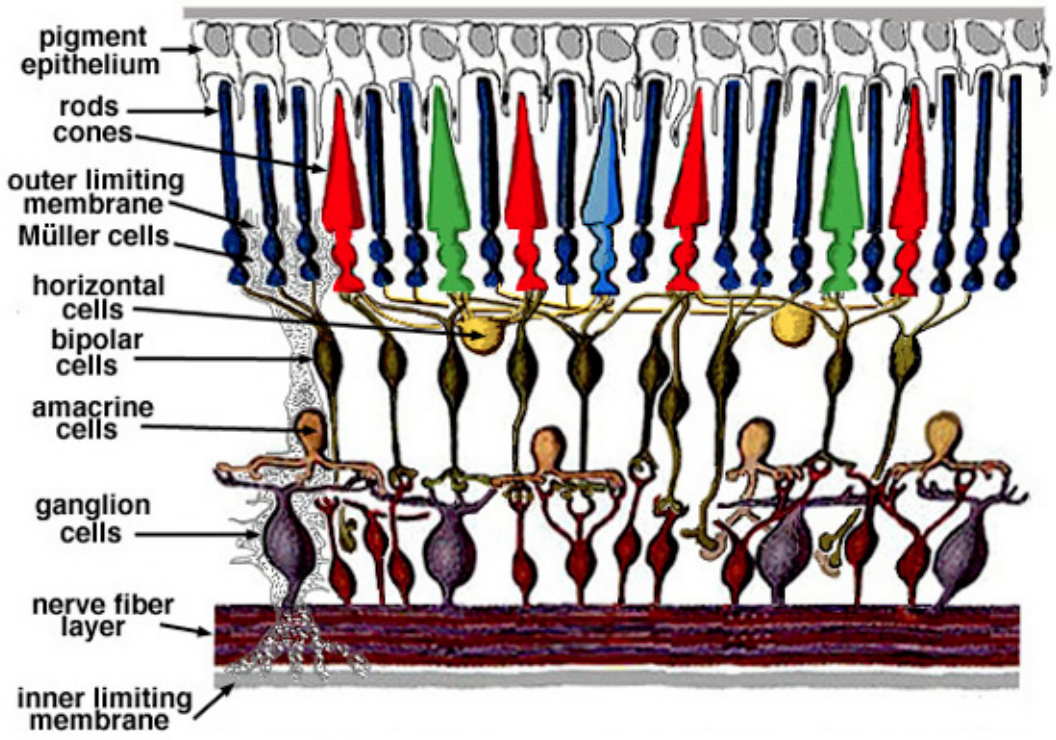

Figure 1: Simplified retina. (Kolb, 2016)

1.1 CELLULAR COMMUNICATION WITHIN THE RETINA

Generally, the mechanisms through which retinal cells 'communicate' are well understood and involve electrical and chemical components. In the most basic example, a cell is composed of dendrites, a soma, and an axon. The soma can be thought of as the main structure of the cell, or the cell body. Here, due to ionic concentrations which are maintained by electrochemical gradients as well as pumps, the cell exhibits a resting polarity of around -70 mV. In order to send a spiking signal, or action potential, the cell needs to become more positive, or depolarized, to around -40 mV through transmembrane interactions and input from other cells. A threshold is reached once this depolarization reaches the aforementioned voltage which opens voltage-gated channels on the cells membrane. These channels allow the influx of positively charged Sodium ions (Na+), or Calcium (Ca2+) ions, into the cell, rapidly creating an electric current across the cell membrane which then propagates along the axon through something called the nodes of Ranvier (Rasband and Peles, 2016), (Hess and Young, 1952). Once this current reaches the tip of the axon, known as the synaptic terminal, neurotransmitters are released into a small gap known as a synaptic cleft, these neurotransmitters then interact with the

receptors on the dendrites of the postsynaptic cell and the process can in theory be then repeated or stopped, depending on if the input is excitatory or inhibitory. (Antkowiak, 2015)

1.1.1 *Photoreceptor Cells*

For this process of cellular communication to take place, there needs to be a trigger that sets it all into action. In the case of the retina, this is light, and photoreceptors are the units responsible for our ability to absorb and transduce light into these aforementioned electrical signals for cellular communication. In general, photoreceptors are able to perform this function due to the presence of a light-absorbing type-2 opsin, *rhodopsin*, which after absorption of light, undergoes a conformational change inducing a cascade of events leading to a change in electric potential. This is known as the signal-transduction pathway and will be covered more in depth later in the introduction. The resultant effect from this pathway interacts with both horizontal and bipolar cells.

Rods and Cones are the two classes of photoreceptors. Though different retinal structures exist throughout the animal kingdom, humans maintain a 1-rod, 3-cone structure (tuned to Short, Medium, & Long wavelengths), while mice have a 1-rod, 2-cone structure in which one cone responds to even shorter, ultraviolet wavelengths and the other corresponds roughly to our M-cone. In general, cones are responsible for color-vision and high-acuity vision. In humans, there exists a 'red-green' pathway created from M-cone vs L-cone center-surround interactions, a 'blue-yellow' pathway created from S-cone vs M-cone/L-cone center-surround interactions, as well as a 'luminosity' pathway which is thought to be the sum of all three cones. Rods are mostly responsible for light sensitivity, representing the only cell type that is active in extremely low light conditions. (Schaffel, 2015), (Münch, Euler, and Baden, 2015)

1.1.2 *Horiztonal Cells*

Horizontal cells act as an intermediate layer between the photoreceptors and the bipolar cells. The main purpose of horizontal cells is thought to be an inhibitory feedback component in which multiple cone outputs are summated and the light response of neighboring cones is reduced. This 'lateral inhibition' is thought to increase responsiveness to edges and decrease responsiveness to uniformly bright objects, this can also be thought of as a form of contrast enhancement. Horizontal cells themselves are connected through gap junctions, which allows quick and efficient communication between cells, granting the functionality to span and communicate over a much larger area than their individual receptive fields. (Wässle, 2004)

1.1.3 *Bipolar Cells*

Bipolar cells (BC) form connections between the inner and the outer retina, and are located between the photoreceptors and the retinal ganglion cells. Mammals have around 12 cone BCs and 1 rod BC. The reasons for the numerous cone BCs are in essence polarity, dynamics, and spectral sensitivity: polarity refers to the ability for a cell to respond through different lighting conditions, dynamics refers to the temporal properties of a response, while spectral sensitivity refers to the cells preference for a specific range of wavelengths of light. Synaptic processes within BCs are probably directly related to the depth at which the BC resides. Furthermore, there are two main types of BC receptors, the OFF ionotropic glutamate receptor (AMPA/Ka), and the ON metabotropic glutamate receptor (mGluR6). Typically, the former ionotropic channel would be considered fast, while the latter mGluR6 would be considered slow. It must also be noted that due to the role that amacrine cells (AC) play in feedback loops, an individual BC can drive two different responses within the next layer of retinal ganglion cells (RGC), but this ability reduces to a single response when the ACs are taken away. Yet, the rod BC does not connect directly to a RGC, and therefore has a connection with a specific amacrine cell, A2, which makes an excitatory electrical synapse with the ON cone BC and an inhibitory glycinergic synapse with the OFF cone BC, after which the process continues onto the RGCs. In order to increase the signal-to-noise ratio to create the best situation for both spatial acuity and light sensitivity, there are three main pathways that the retinal system uses which involve the BCs according to different light conditions: in low-light scotopic conditions, the previously mentioned rod BC pathway is utilized, in twilight mesopic conditions, a direct electrical coupling between rods and cones is utilized, and in day-light photopic conditions, the cone pathway to the RGCs is more fully utilized. These connections with the RGCs take on different forms as well, on one hand we have spiking BCs, which typically make synapses with several RGCs, and on the other we have analog graded BCs, which typically make a single synapse with a RGC. Taken altogether, BCs are a crucial switchboard-like component that sorts and manipulates information from the photoreceptors, and then passes it into the proper ganglion cell channels. (Schaffel, 2015), (Münch, Euler, and Baden, 2015)

1.1.4 *Amacrine Cells*

Amacrine cells (AC) are mostly inhibitory components that are nestled in the range of bipolar cells and retinal ganglion cells. So far, about 20-30 types have been found, but our understanding is limited to perhaps 5: the A2 cell, the A17 cell, the Starburst AC, the polyaxonal AC, and the Dopamine AC. Briefly, A2 is thought to be mostly involved in center-surround properties of ganglion cells while also serving as a pathway between rod bipolar cells and retinal ganglion cells, A17 is thought to be involved in gain control through very localized feedback circuitry between ON rod bipolar cells and the A2 AC, the Starburst AC is thought to be involved in direction selectivity, the polyaxonal AC is thought to be involved in object segregation and suppression of global motion, while Dopamine ACs are thought to play a central role in "reconfiguring retinal function" with respect to illumination conditions. (Schaffel, 2015), (Münch, Euler, and Baden, 2015), (Zhang et al., 2008)

1.1.5 *Retinal Ganglion Cells*

Retinal ganglion cells (RGC) represent the last layer in retinal processing, and their axons are the connection between the retina and the first relay in the brain, the lateral geniculate nucleus (LGN). Most RGC types are thought to form a mosaic type structure in which there is little overlap between cells, but is an organization which spans the entire retina. We have categorized about 10-15 types of these ganglion cells based on morphological components, functionally, there is less known. With that being said, there is basic experimental evidence regarding the functioning of the Alpha (parasol) RGCs, Beta (midget) RGCs, direction-selective RGCs, color-coded RGCs, and Melanopsin-containing RGCs. Alpha RGCs are thought to function as Brisk Transient (Y) cells which have both ON and OFF varieties, these cells have fast activation times, and are thought to be something of a 'visual switch' which calls for visual attention. Furthermore, they are particularly acute for sensations of small, jerky movements, flickering stimuli, as well as second-order contrast modulations within drifting motion stimuli. Beta cells, due to their one-to-one connectivity are generally thought to be most completely involved in high-acuity vision and spatial resolution. Additionally, this midget RGC pathway is thought to be involved in the transmission of the opponent pathways which are responsible for color vision. Directional-selective cells are thought to encode direction through an excitatory-inhibitory push-pull type of mechanism. Lastly, Melanopsin-containing RGCs are thought to represent a small proportion of RGCs, but are nevertheless vital to circadian rhythms, the pupillary reflex, and encoding ambient light levels. (Schaffel, 2015), (Münch, Euler, and Baden, 2015), (Wässle, 2004)

1.2 THE VISUAL PATHWAY

The pathway from light sensation to perception has many components. Once the information from the retina is processed, it is relayed through axons of the RGCs into the LGN and onto the visual cortex. Intricate and complex processing, as seen in figure 2, occurs within the LGN and throughout the cortex, eventually leading to visual perception. The complete scope of visual perception is outside of the realm of this thesis, but it should be noted that each layer of processing seems to have dedicated information extraction and manipulation components which altogether create our view of the world.

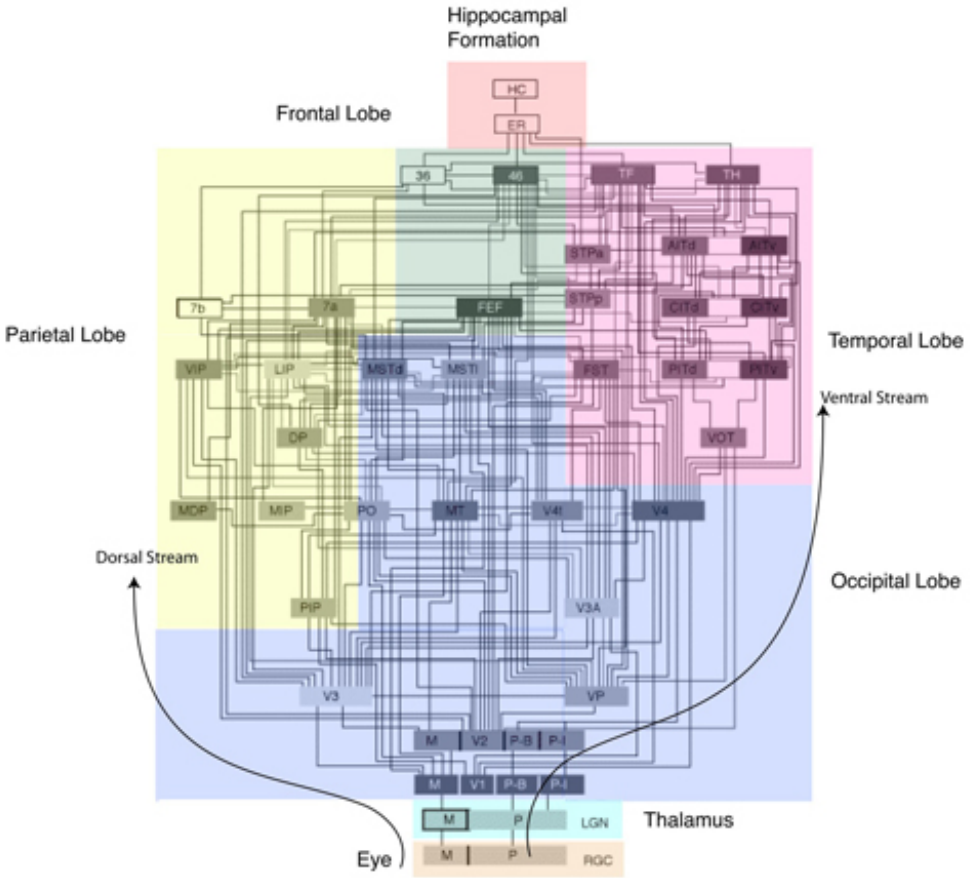

Figure 2: Visual Processing Network, from eye to cortex.
Image originally by (Felleman and Van Essen, 1991),
recreated by (Rokem, 2007)

2

INTRODUCTION

Vision is an essential tool for the exploration of our environment. Clearly, changes in our visual environment can elicit changes in our behavior: examples range from being scared when something unexpectedly pops out at you, to the stillness when examining a painting of interest, or even the saccades that our eyes make while gazing out of a train window. Humans rely on vision to carry out many facets of daily life, yet estimates for the prevalence of complete or partial blindness resulting from retinal diseases such as retinitis pigmentosa are 1 in 4000 people (Hartong, Berson, and Dryja, 2006), with the prevalence increasing to 1 in 300 people with the addition of age-related macular degeneration and diabetic retinopathy (Wyk et al., 2015). These retinal degenerative diseases are the result of genetic mutations leading to progressive photoreceptor loss (Mutter, Swietek, and Münch, 2014). This thesis will explore vision restoration in the context of behavioral assessment through innovative optogenetic approaches.

2.1 THE SIGNAL TRANSDUCTION PATHWAY

After light enters the eye, it must pass through the bipolar and retinal ganglion cell layers of the retina before falling upon the photoreceptor layer. Photoreceptors in particular are the light transducing mechanisms through which the phototransduction cascade that eventually leads to perceptual vision begins. This layer consists of two main cell types, cones and rods, the former being heavily involved in color vision and acuity, while the latter is heavily involved in light sensitivity. Each of these cell types has a specific range of sensitivities to different wavelengths, a tuning curve. This typically bell-shaped tuning curve in practical terms means that the cell responds greater to wavelengths that fall in the peak sensitivity range than those that fall outside of such. Counterintuitively, photoreceptors maintain what is known as dark current, which means that the cell is excited, or depolarized, to about -40mV in the dark through a process that allows Na+ ions to flow into the cell through cyclic GMP (cGMP) gated channels (Kandel et al., 2000). Now, once a wavelength of light within the tuning curve falls upon the photoreceptor, the signal transduction pathway is activated, involving a series of events and signal amplifications which lead to a change in the membrane potential of the cell. First, the opsin of rhodopsin, located in the disc membrane of the photoreceptor outer segment, absorbs a photon, causing a conformational change in the rhodopsin through the chromophore 11-cis retinal by its photoisomerization into another form called all-trans retinal. This conformational change then goes on to activate a G-protein called transducin, through which a signal amplification of about 100x occurs, in

that each photoactivated rhodopsin triggers activation of approximately 100 transducins. Each transducin activates the enzyme cGMP-specific phosphodiesterase (PDE). PDE is involved in the hydrolysis of cGMP into 5′ GMP, which is also the second amplification stage, in which each PDE catalyzes the hydrolysis of approximately 1000 cGMP molecules. Due to this chemical breakdown of cGMP, the net concentration of such is lowered, resulting in the closure of the aforementioned cGMP gated Na+ channels. This reduction in the positive influx of Na+ ions into the cell causes the cell to hyperpolarize at a rate of about 2mV *per single photon* due to the 1 : 1,000,000 amplification process. This reduction in cell membrane potential leads to the closure of voltage-gated Ca2+ channels, while the reduction in Ca2+ reduces the exocytosis of glutamate to the bipolar cell. Importantly, reduction in glutamate flow results in two distinct events depending on the bipolar cell receptor: in metabotropic bipolar cells (ON bipolar cells) there is a depolarization, and in ionotropic bipolar cells (OFF bipolar cells) there is a hyperpolarization. These bipolar cells then pass the signal to ON and OFF retinal ganglion cells, respectively, through a variety of different synapses, with interactions from amacrine and horizontal cells. Retinal processing is thought to take into account the spectral properties of light (Wässle, 2004), object and background motion (Ölveczky, Baccus, and Meister, 2003), light intensity (Reinhard et al., 2015), (Smirnakis et al., 1997), and directional motion (Fried, Münch, and Werblin, 2002), among other features, before passing through the optic nerve and onto higher levels of visual processing such as the lateral geniculate nucleus and the visual cortex (Schaffel, 2015), (Münch, Euler, and Baden, 2015), (Kandel et al., 2000), (Ebrey and Koutalos, 2001), (Leskov et al., 2000). For extensive review of all retinal components and connections, see (Wässle, 2004).

2.2 THE RETINAL DEGENERATION MODEL

Despite this complex and extensive retinal architecture, a loss of only the light transducing photoreceptors renders the entire system dysfunctional. This loss of functionality is realized within the aforementioned diseases of retinitis pigmentosa or macular degeneration. In order to better determine how we can clinically treat these diseases, two models of the retinal degeneration present in retinitis pigmentosa are commonly used within the mouse, *rd1* and *rd10*. The model used in the study at hand is *rd1*, developed by Keeler in 1966 (Keeler, 1966). Rd1 invokes early and severe retinal degeneration due to a murine viral insert and a nonsense mutation in exon 7, as well as a second nonsense mutation within the beta subunit of the rod-specific phosphodiesterase gene, which has also been shown in human counterparts with retinitis pigmentosa (Chang et al., 2002). This disease is characterized by a complete loss of the rod photoreceptors from postnatal day (P) 30, followed by a slower degeneration of the cone photoreceptors (due to reasons unknown, as the mutation is only within the rod photoreceptors), as well as a remodeling of the

remaining retinal structure (Pennesi et al., 2012), (Lin, Masland, and Strettoi, 2009). This slower degeneration found within the cones has been reported to be almost complete as early as P120 (Lin, Masland, and Strettoi, 2009).

2.3 THERAPEUTIC APPROACHES

As a result of photoreceptor loss leading to blindness, several research groups have focused directly on slowing photoreceptor degeneration through either pharmacological methods (Beltran, 2008), or gene replacement therapies (Bainbridge et al., 2008),(Busskamp et al., 2014). Yet, these methodologies rely on early detection of photoreceptor degeneration, and therefore are generally too late in the time frame to be considered in current clinical framework in which patients only realize the degeneration after photoreceptor death has progressed significantly (Wyk et al., 2015). Due to this, a second group of therapeutic treatments emerge which seek to tap into the remaining visual architecture, such as: retinal implants (Zrenner et al., 2011), (Rizzo and Wyatt, 1997), stem cells (Li et al., 2013), (Santos-Ferreira et al., 2015), photochemical ligands (Polosukhina et al., 2012), ectopic expression of native human rod opsin (Cehajic-Kapetanovic et al., 2015), and optogenetics (Wyk et al., 2015), (Lagali et al., 2008), (Busskamp et al., 2010). While the other methodologies hold merit, to include them all is beyond the scope of this thesis, and therefore the following will focus solely on the optogenetic approach.

2.4 OPTOGENETICS

The main idea of optogenetics is to restore the phototransducing component of the visual system by introducing light sensitive proteins into the retina (Mutter, Swietek, and Münch, 2014). One of the first and most widely used proteins is Channelrhodopsin-2 (ChR2), discovered in the unicellular algae *Chlamydomonas reinhardtii* (Nagel et al., 2002), (Nagel et al., 2003). These algae primarily use this light sensitive protein as a means to increase photosynthesis: by sensing where light is coming from they can then orient and move toward it. ChR2 represents the light sensitive protein used in this situation. It can be extracted and expressed in another cell type, even in another organism and environment, like the human or mouse retina. ChR2 acts as a light-gated, unselective cation channel with conductance for H+, Na+, K+ and Ca2+ ions, with the influx of these positive ions resulting in a depolarization of cells to the peak wavelength of 470nm (Nagel et al., 2003). ChR2 has been expressed in both bipolar cells (Lagali et al., 2008) and ganglion cells (Bi et al., 2006), and has been shown to restore stimulus-driven electrical activity within the mouse retina in both cases. Another optogenetic protein is Halorhodopsin (NpHR), which unlike the depolarizing effect of ChR2, has a hyperpolarizing effect to the peak wavelength of 580nm (Lanyi, 1990), (Fenno, Yizhar, and Deisseroth, 2011). NpHR has been expressed in the cone photoreceptors and has also been shown

to restore electrical activity within the mouse retina (Busskamp et al., 2010). Most recently, in 2015 Kleinlogel et al. (Wyk et al., 2015) developed a novel optogenetic tool, Opto-mGluR6, which was created through manipulations within the intracellular loops of the metabotropic glutamate receptor 'mGluR6' of the ON-bipolar cell, and the likewise native light-sensitive protein melanopsin, which has a peak sensitivity of 467nm. This protein is activated directly by light, and due to the sign inverting properties of mGluR6, causes the ON-bipolar cells to hyperpolarize. This is a reversed polarity when compared to the native functioning of mGluR6, which causes the ON-bipolar cells to depolarize in light. Furthermore, Opto-mGluR6 has been successfully shown to restore basic ecologically-relevant and visually-driven behavior through tasks such as the Optokinetic Reflex Drum and Water Maze, as well as stimulus-driven electrical activity in ON bipolar cells, ON and OFF retinal ganglion cells, and V1 through patch clamp, in vivo optical imaging, and electrophysiological methods. Opto-mGluR6 was also reported to be 1 to 2 log units more light sensitive than even the best ChR2 variants due to signal amplification created by tapping into the pre-exisiting G-protein cascade with RGS/TRPM1-complexes (Wyk et al., 2015). This is important because the visual system maintains a dynamic range of light responses over 12 orders of magnitude (10^4 to 10^{16} photons $s^{-}1cm^{-}2$) (Hood and Finkelstein, 1986), and the minimum activation threshold for ChR2 is roughly around 10^{15} photons $s^{-}1cm^{-}2$ (Lagali et al., 2008), (Doroudchi et al., 2011), which means even at optimum conditions ChR2 can only encode approximately 1 order of magnitude, therefore encoding light responses for approximately 8.33 % of the normal dynamic range. On the other hand, the minimum activation threshold of Opto-mGluR6, as reported by (Wyk et al., 2015), is around 5 x 10^{11} photons $s^{-}1cm^{-}2$, which means with optimum conditions Opto-mGluR6 can encode approximately 4.3 orders of magnitude, therefore encoding light responses for 35.8 % of the normal dynamic range. Furthermore, this difference in minimum activation level is important because such high light intensities as needed by ChR2 are rare in nature, and sustained intensities of such have been shown to be toxic to the retina (Hunter et al., 2012). As patients suffering from a retinal degenerative disease generally maintain some photoreceptors, jeopardizing their health to activate ChR2 is seemingly unproductive. When simply only taking this single fact of activation threshold into account, Opto-mGluR6 seems to be better suited for clinical interventions than its widely used ChR2 counterpart.

2.5 BEHAVIORAL ASSESSMENT

With these optogenetic proteins in mind, we can think to assess their visual restorative properties through different mechanisms. Relatively objective measures that come from electrophysiological, microscopy, and histology techniques are useful for measuring if there are indeed characteristic light responses which would constitute a restoration of the visual pathway by being present in downstream retinal

cells or even higher visual processing areas, as well as how well the protein was expressed in the targeted cells (Lagali et al., 2008). Yet, we are not able to construct exactly what these cellular responses mean in the terms of ecologically relevant vision with our current understanding of how the optogenetic proteins integrate and function within the retinal circuitry, therefore it is imperative that any visual restoration treatments are also assessed in the behavioral realm. Van and Kleinlogel (Wyk et al., 2015) attempted to further validate the successful integration of Opto-mGluR6 into the retinal processing architecture by conducting two main behavioral paradigms: the "Optokinetic Reflex Drum" and the "Water Maze". While these behavioral assessments are important, I attempted to expand the assessment by focusing on measuring five prototypical and visually induced behavioral states: aversion, attraction, excitation, inhibition, and evolutionarily-based reactions. In order to access these behavioral states, three main paradigms were used: "The Box", modeled from (Cehajic-Kapetanovic et al., 2015) and the review from (Bourin and Hascoët, 2003), which allowed stimulus presentation on two monitors, creating situations to measure aversion, attraction, excitation, and inhibition; the "Optokinetic Reflex Drum", which allowed measurements of visual acuity and contrast sensitivity through a displayed reflexive movement (Benkner et al., 2013); and the "Looming Stimulus", which allowed measurements of evolutionarily-based reactions to a potentially threatening stimulus. Stimuli were chosen based on established literature of mouse behavior, such as the light-avoidance displayed in the light/dark paradigm (Bourin and Hascoët, 2003), (Takao and Miyakawa, 2006), the looming stimulus flight or freeze response (Yilmaz and Meister, 2013), (Wallace et al., 2013), (Münch, 2013), the optokinetic reflexive movement to drifting gratings (Mitchiner, Pinto, and Vanable, 1976), (Douglas et al., 2005), or activity changes when exposed to a flicker (Cehajic-Kapetanovic et al., 2015). The general idea for these behavioral experiments is simple: record a control behavior which was gathered through measurements taken during a control period, and then compare such to the displayed behavior during the stimulus period.

3

METHODS

One major goal of this project was to determine the behavioral relevancy afforded by the addition of an optogenetic component to an rd-1 degenerating retina. In order to examine this question in further detail, three main behavioral paradigms were used: "The Box", the "Optokinetic Reflex Drum", and the "Looming Stimulus". The behavior for each paradigm was recorded by its own camera setup: for "The Box", the camera was mounted overhead and the X/Y coordinates of the mouse were tracked through BioBServe software; for the "Optokinetic Reflex Drum", the camera was mounted overhead and custom made software segmented the mouse head, body, and tail and calculated a directional vector of the head with respect to the body in order to track optokinetic pursuit movements (Benkner et al., 2013); for the "Looming Stimulus", the camera was mounted within the box and behavior was recorded by hand post-experimentally and then analyzed through custom MATLAB and Mathematica codes. In addition to these measures, attention was paid to the brightness of the testing room, the monitor settings, the cleaning protocol, as well as possible acoustic emissions emanating from the monitors.

3.1 GROUPS

Behavioral comparisons were made between five distinct mouse groups:
•Group 1 (Albino WT, n = 6): CD1 albino background (does not contain rd1 mutation)
•Group 2 (Albino ChR2, n = 5): transgenic L7-ChR2-eYFP mice on a CD1 albino background (contains rd1 mutation and ChR2 expression in ON bipolar cells)
•Group 3 (Albino rd1, n = 5): CD1 albino background (contains rd1 mutation)
•Group 4 (Bern Opto-mGluR6, n = 7): FVB/Opto-mGluR6 crossed with C3H/HeOu mice, leading to mice with rd1 and Opto-mGluR6 expression in ON bipolar cells.
•Group 5 (Bern rd1, n = 4): FVB/Opto-mGluR6 crossed with C3H/HeOu mice, leading to mice with rd1

Mice were housed in cages with no more than 2 littermates. The mouse habitat consisted of a 12-hour light / 12-hour dark cycle, minimal handling, free-access to water and food, and kept in a room with other mice cages. The light intensity levels of the home room measured to be 1600 lux from a distance of 1m away from the light source and 500 lux from the distance of the cages, while the intensity levels

of the experimental room measured to be 500 lux from a distance of 1m away from the light source and 175 lux from the distance of the cages. These measurements were taken with the light sensor oriented with the maximal absorption angle.

3.2 "THE BOX"

"The Box" is a trapezoidal area measuring 79cm x 48.6cm x 57cm x 48.6cm (with a 35cm high ceiling) which is separated into two zones by a wall which left an 8.6cm open cross-over area (figure 3). Each zone was fit with computer monitors that primarily could only be seen in their respected zones. Within the setup, four main stimuli were used: full-field illumination changes, flickers, drifting gratings, and the light/dark box paradigm (Bourin and Hascoët, 2003), (Takao and Miyakawa, 2006).

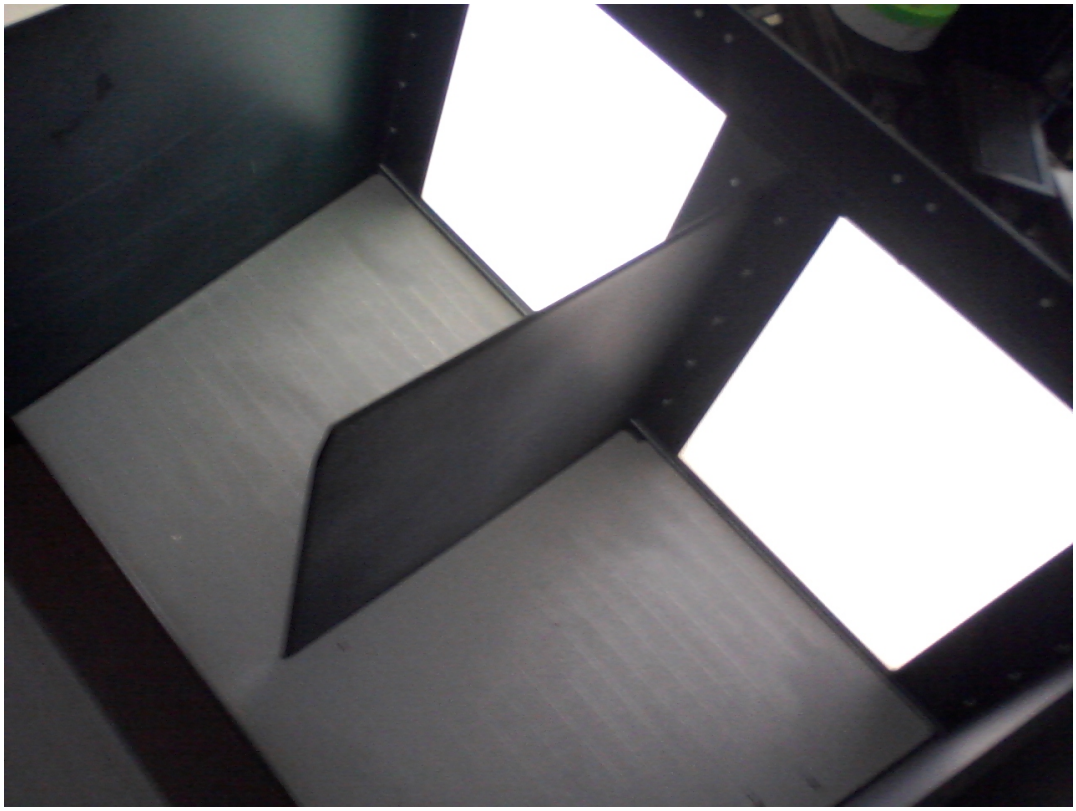

Figure 3: Image of "The Box". Own source.

3.2.1 *Habituation Protocol*

Before any experiments were conducted, a 10-day habituation protocol broken into two parts was first conducted. In part one, the mice were accustomed over 5 days to the testing room in their home cages for 30-minute periods. The second 5-day habituation protocol also involved leaving the mice to acclimatize to the testing room over 30 minutes, following which the mice were placed for the first 3 days within the box with their cagemates for 10-minute periods with neutral grey screens (in preparation for flicker or drifting grating experiments) or black screens (in preparation for full field or light/dark experiments), with a rotating cage sequence. On the 4th and 5th day, the same protocol was followed with the difference being that each individual mouse had 10 minute periods in the box by themselves. To avoid olfactory cues, the arena was thoroughly cleaned with 70% Ethanol and allowed to air dry between every instance where a mouse came into contact with a surface. Following this 10-day habituation protocol, each experimental day began with a 30-minute acclimatization to the testing room.

3.2.2 *Experimental Protocol*

After the habituation period, a mouse was placed into the box for a 5-minute period where the control screens were displayed, after which the specific experimental protocol began. Between mice, the box was thoroughly cleaned with 70% Ethanol and allowed to air dry between every instance where a mouse came into contact with a surface. Only one experiment of any kind was conducted per day.

3.2.3 *Full Field Illumination Protocol*

After the control time displaying black screens elapsed, a MATLAB code triggered a full field illumination change on both monitors to maximum white for 1 minute, where after both screens then again displayed black for 1 additional minute. Both the Albino and Bern mice groups were P240, on average.

3.2.4 *4Hz Flicker Protocol*

After the control time displaying gray screens elapsed, a MATLAB code took into account the XY position of the mouse and then triggered a 4Hz flicker within the zone that the mouse was in, while the other screen maintained the control gray screen. This stimulus lasted for 1 minute, where after both screens then again displayed the neutral gray for 1 additional minute. Albino mice were P237, on average, while the Bern mice were P230, on average.

3.2.5 *Drifting Grating Protocol*

After the control time displaying gray screens elapsed, a MATLAB code triggered drifting gratings on both screens at the speed of 1.2 cycles per second and the resolution of 0.1 cycles per degree, or 5.4cm per cycle in physical width. This stimulus lasted for 1 minute, where after both screens then again displayed the neutral gray for 1 additional minute. Albino mice were P240, on average, while the Bern mice were P220, on average.

3.2.6 *Light/Dark Box Paradigm*

After this control time displaying black screens elapsed, a MATLAB code took into account the XY position of the mouse and then triggered a 100% intensity white screen within the zone that the mouse was in, while the other screen maintained the control black screen. This stimulus lasted for 1 minute, where after both screens then again displayed black for 1 additional minute. Albino mice were P250, on average, while the Bern mice were P240, on average.

3.3 THE "OPTOKINETIC REFLEX DRUM"

The "Optokinetic Reflex Drum" is a box in which the 4 walls consist of computer monitors, along with a mirrored ceiling and floor to make a complete surrounding effect, as seen in (figure 10). The mouse sits on a raised platform surrounded by a flexible wire, which reduces the tendency to climb off of the platform. Depending on the position of the mouse, the width of the stripes are manipulated to maintain a constant resolution (figure 10). Once the mouse is still, defined by no changes in body coordinates measuring more than 0.03cm for at least 0.25s, the stimulus then displays for at least 1s, and at most 5s, terminated prematurely if body movement exceeding 0.3cm is measured. In a single trial, the total stimulus presentation must either exceed 35s and have equal presentations of counter-clockwise and clockwise rotation, or have a positive detection of the optokinetic reflex behavior. Only the Bern mice were tested in this paradigm.

3.3.1 *Habituation Protocol*

Mice entering the Optokinetic Reflex Drum have already undergone prior experiments, and therefore were pre-exposed to the testing room and experimental requirements. Nevertheless, each experimental day began with a 30-minute acclimatization to the testing room.

Figure 4: Photograph taken of the inside of the OptoDrum, from (Benkner et al., 2013)

3.3.2 *Experimental Protocol*

After the acclimatization period, the mouse was placed on the raised platform with a presentation of gray screens for 1-minute. Following this time, the experimental protocol was activated. Meaning the movement of the mouse was measured and the stimulus was displayed when the aforementioned conditions were met. The stimuli were broken into two categories: resolution and contrast. At first exposure, all mice were given the resolution condition of 0.05 cycles per degree (cpd) at 100% black and white contrast. To receive a "fail" of the condition, the mouse was required to display no optokinetic reflexive behavior for 3 successive trials. To receive a "pass" of the condition, the mouse was required to display the tracking behavior. Once this behavior was displayed, the resolution remained the same, but the contrast was dropped below 100% in the following step-wise manner until a "fail" was received: 50%, 75% (only if 50% = "fail"), 25%, 20%, 15%, 10%, 9%, 8%, 7%, 6%, 5%. After the minimum contrast for 0.05 cpd resolution was established, the resolution was shifted to finer conditions in the following manner: 0.06 cpd, 0.15 cpd, 0.35 cpd. Trials were conducted at P232, P272, and P307.

3.4 THE "LOOMING STIMULUS"

The "Looming Stimulus" paradigm was conducted in a trapezoidal area measuring 57cm x 40cm x 37cm x 40cm (with a 35cm high ceiling). The ceiling had a square cutout fitted with a computer screen measuring 25cm x 30cm. The setup also contained a familiar red plexiglass shelter. The stimulus itself was either a white or black expanding disc, to mimic the exponential expansion that would occur in real life if a predator were to descend upon you from the sky, the disc was modeled with the formula: radius = $2000(\mathrm{atan}(60t - 120) + \pi/2) + 10$, as seen in figure 5, with a radius given in pixels, and time 't' in seconds. During the presentation in the current study, the disc completed 15 expansions over 30 seconds, in which each expansion started as a 10 pixel disc and ended after the complete screen was covered. Only the Bern mice were tested in this paradigm.

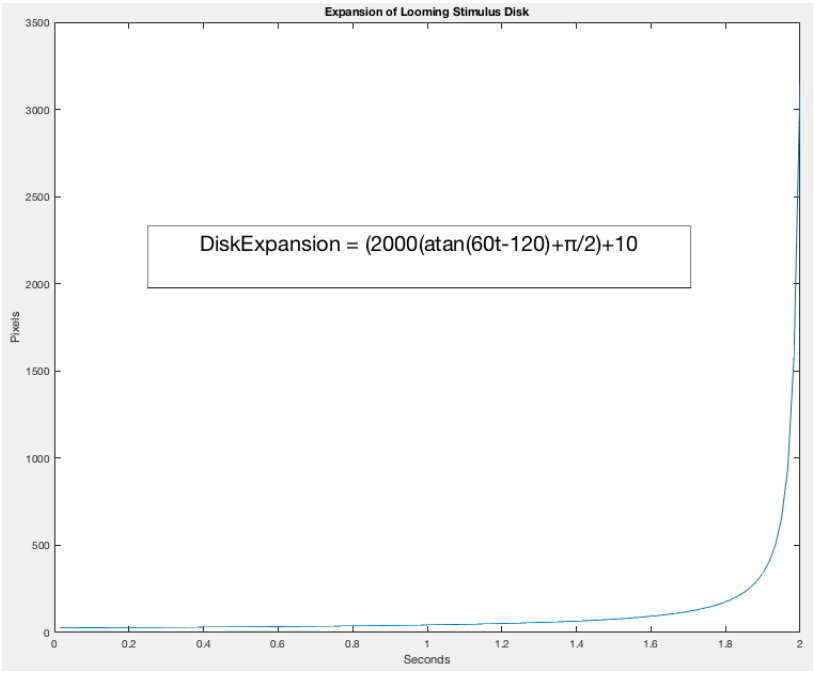

Figure 5: Disk increase as a function of pixels over time

3.4.1 *Habituation Protocol*

Each mouse underwent a 3-day habituation without stimuli before the experimental condition. After 30 minutes of testing room acclimatization, mice were placed into the box with their cagemates for the first 2 days for a total of 10 minutes per day, and were individually placed in the box for 10 minutes on the 3rd day. During this time, a neutral gray screen displayed overhead, and the mice explored the box as well as the red plexiglass shelter located there within. Between mice, the arena and the shelter were cleaned thoroughly with 70% Ethanol and allowed to air dry. Following this 3-day habituation period, each experimental day began with a 30-minute acclimatization to the testing room.

3.4.2 *Experimental Protocol*

After the acclimatization period, the mouse was placed in the arena for a 5-minute control period while a neutral gray (or dark gray) screen was displayed. Following the control period, the stimulus of either a black or white expanding disc was initialized if the mouse met the two conditions of being out of the shelter and within a visual trigger zone under the screen. A total of 5 experimental days were conducted as follows:

- Black disc [0 0 0] on gray background [127 127 127] (P225)
- White disc [255 255 255] on gray background [100 100 100] (P230)
- Black disc [0 0 0] on gray background [127 127 127] (P235)
- White disc [255 255 255] on dark gray background [20 20 20] (P270)
- Black disc [0 0 0] on gray background [127 127 127] (P275).

3.4.3 *Behavioral Analysis*

Post-experimental analysis of each mouse's behavior was conducted using a custom MATLAB script to record key presses as High Definition recordings of the mice were watched by a trained observer (myself). Recorded behaviors of interest included: stillness, walking, flight, rearing on wall, rearing in open, going in to the shelter, going out of the shelter, and back pedaling. This resulted in a visualization of each behavior through time, as seen in figure 6. The encoded behavior was then analyzed through a custom Mathematica script. First, within a sliding window of 10-second duration, the behavior was analyzed as follows: the duration of occurance of each behavior within each window was expressed as a percentage of the total duration of this behavior. The 10-second window was then shifted by 1 second and the process repeated. If a certain behavior (e.g., flight) occurred only once, this would result in a value of "100%" if the 10-second analysis window contained that single event, and "0%" if not. If a behavior was commonly observed, this would result in lower percentage values throughout the analysis. Four behaviors were chosen for analysis and mapped onto 3-axes, chosen as follows: one axis representing 'stillness', one axis representing 'exploratory rearing', and one axis representing both 'flight' and 'back pedaling' (as they are particularly unique behaviors). These behavioral axes were chosen subjectively and on the basis that they could best capture reactions to the looming stimulus if they should be present, according to literature reports (Yilmaz and Meister, 2013), (Wallace et al., 2013), (Münch, 2013). Each point within this 3-axes space represented a single 10-second window and had the coordinates of the calculated percentage values for each of the behaviors. Within this point cloud, the *behavioral uniqueness* of each point was calculated through its vector distance to the median centroid of all other 10-second interval values. In general, this determines how similar a single point is compared to the group; if a point was far away from all other points it would have a high behavioral uniqueness value. These behavioral uniqueness values were then compared to all other behavioral uniqueness values, finding the intervals where the behavior was most unique. In figure 7, the 10-second analysis windows that contained the looming stimulus are color-coded in orange, and all the rest are blue. It is obvious that in this example, the mouse's behavior is distinct while the looming stimulus is displayed.

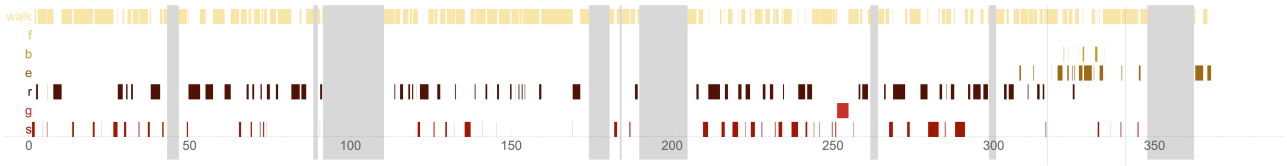

Figure 6: Rows display the following behaviors in descending order: walking, flight, back-pedaling, exploratory rearing, rearing, grooming, and stillness. Gray sections represent time inside shelter. Vertical black lines seen between 315s-345s represent stimulus onset and offset.

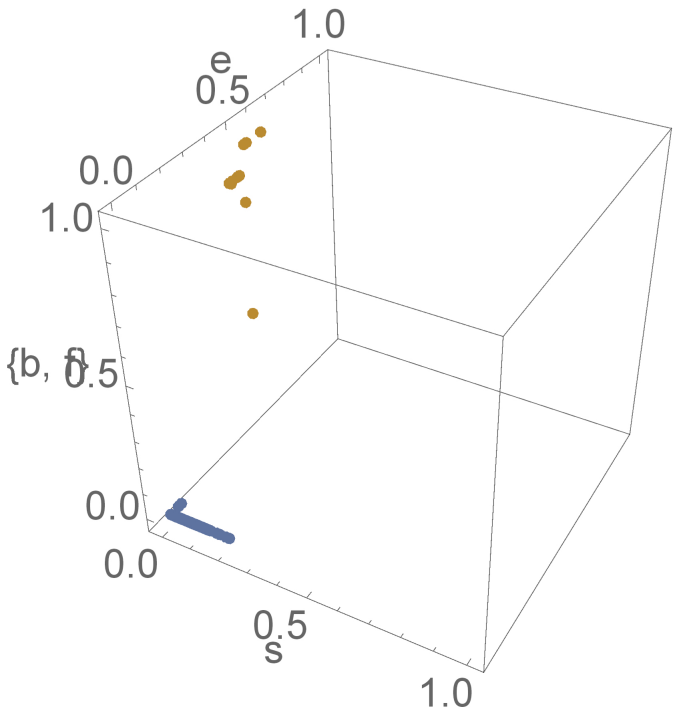

Figure 7: Point cloud representing displayed behaviors within intervals. Blue represents control intervals, orange represents stimulus intervals. "e" represents exploratory rearing. "s" represents stillness. "b, f" represent both back-pedaling and flight behavior. Numbers represent percentage of that behavior within a single interval compared to the total behavioral occurrence.

3.5 EQUIPMENT

Eizo EV2450-BK Monitors: The experimental monitors were first calibrated with a ThorLabs S120B Intensity Sensor affixed directly to the monitor screen, connected to a ThorLabs PM100 Optical Power Meter System to obtain measurements of screen intensity in µW. The screen was stepped down from maximum intensity white [color code: 255 255 255, contrast 100%] in increments of 5 until 210 210 210, where then increments were increased to 10 until 50 50 50, where then increments were placed back at 5 until minimum intensity black [0 0 0] was displayed. A measurement of intensity was taken at each increment. To create monitor settings which placed neutral gray in between the maximum white and minimum black intensity values, a custom Mathematica code "gammaCorrection" was used. After these levels were established, as seen in (figure 9), all reported contrast levels were scaled to the monitor settings according to this neutral gray. This was tested by displaying single-pixel width black and white stripes on each monitor and checking if they equaled the values emitted by neutral gray, in addition to a manual visual inspection in respect to the scales found on the "National Archives and Records Administration Monitor Adjustment Target" (figure 8). Furthermore, these levels were established with the contrast and brightness of the internal monitor settings of 58 contrast and 100 brightness.

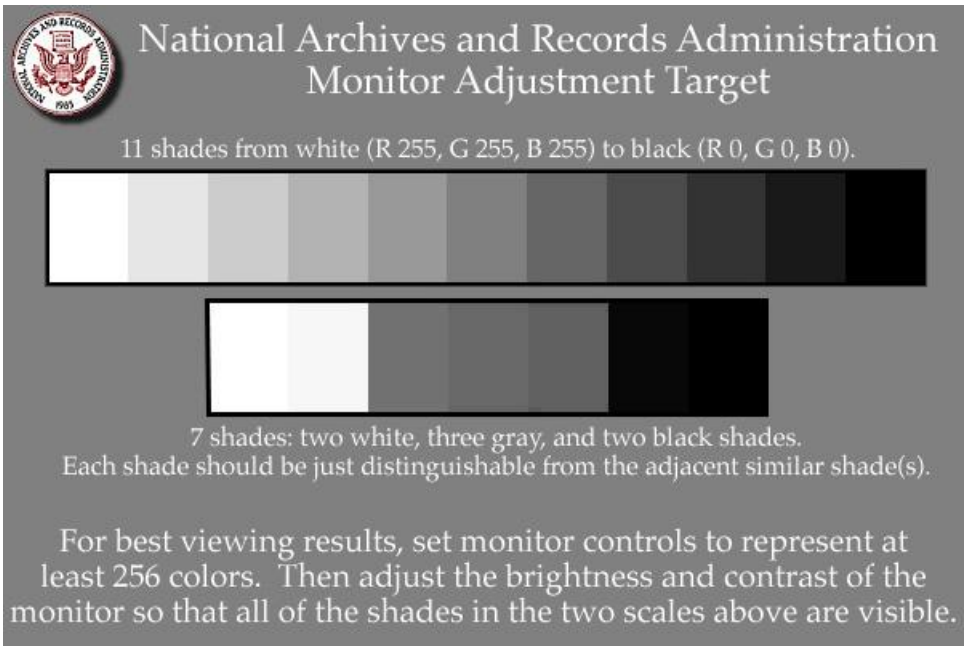

Figure 8: Manual inspection of contrast scale

Helligkeit	Monitor 1	Monitor 2	
255	292	290	µW
250	283.2	280.8	
245	266.2	261.7	
240	252.9	248.3	
235	243.5	239.2	
230	233.2	229.7	
225	222.9	219.2	
220	211.1	209	
215	201.7	201.6	
210	193.9	193.2	
200	178.6	178.9	
190	166.1	165.4	
180	155.2	154.5	
170	145.5	145.2	
160	136.2	135.7	
150	128.2	127.2	
140	120.5	119.3	
130	114.3	113.3	
120	108.2	107	
110	102.8	101.2	
100	97.39	95.9	
90	92.83	91.2	
80	88.88	87.17	
70	85.53	83.62	
60	82.29	80.52	
50	79.06	77.3	
45	77.67	75.92	
40	76.31	74.56	
35	75.31	73.49	
30	74.29	72.57	
25	73.37	71.68	
20	72.48	70.81	
15	71.55	69.95	
10	70.83	69.28	

		Distance from Light Source	
		100cm	**Cage Position (~200cm)**
Rooms	Home Room	1600 lux	500 lux
	Experimental Room	500 lux	175 lux
		5cm	**Back of Zone (~40cm)**
Screen Values	0 0 0	10 lux	8 lux
	75 75 75	169 lux	82 lux
	127 127 127	330 lux	170 lux
	180 180 180	750 lux	290 lux
	200 200 200	780 lux	320 lux
	255 255 255	1100 lux	480 lux

Figure 9: Left: Light measurements taken from two monitors used in the behavioral experiments for calibration purposes. Monitor values listed are in micro-watts, the sensor was affixed directly to the monitor screen.
Right: measurements (in lux) were taken from the mentioned distances.

G.R.A.S. Sound & Vibration High-Frequency Ultrasonic Microphone and Pre-Amplifier type 26AM: To determine whether a potential confounding variable occurred from acoustic emissions from the monitors themselves, specifically during stimulus administration, this microphone was placed approximately 10 centimeters away from the monitor and set to record with a sampling rate of 250,000 Hz. Recording was done both in isolation and during experiment in order to both record potential emissions as well any ultrasound communications from the mice themselves. This microphone was used in combination with a G.R.A.S Power Model type 12AK. A power-spectrum analysis showed no noticeable differences in acoustic emissions between control and stimulus periods.

Matrix Vision Blue Fox Inline Camera / VIDO B&W CCD Inline Camera / GoPro Hero 4: Inline cameras directly connected the computer were set for both the Optokinetic Reflex Drum (Matrix Vision) as well as The Box (VIDO). The GoPro Hero 4 was used during the looming stimulus in order to obtain high definition videos that could later be analyzed for behavior.

Camera Optics: Additionally, an HF 3.5M-2 Fixed Focal Lens of 1/2" C 3.5mm F1.6 was used with the VIDO inline camera. An infrared filter was used in some cases depending on detection quality due to differences in mouse fur color.

940nm Infrared LED Strip from Solarox: This lighting strip was placed along the edge of the ceiling in order to illuminate the experimental arena for better detection from the camera systems.

OptoDrum: This Optokinetic Reflex Drum setup was used to measure contrast sensitivity and visual acuity as described in (Benkner et al., 2013). It can be purchased through contact with:
info@striata-tech.com

Lux Light Sensor: This sensor was found within the hardware of the Samsung Galaxy S5, as accessed by the input "*#0*#", and then choosing "light sensor".

3.6 SOFTWARE

BioBServe Software: This software created a representation of the centroid point of the mouse through a video feed supplied by the aforementioned camera. Positional changes were measured over 4 millisecond intervals. This software can be found at:
http://www.biobserve.com/

MATLAB Software: This software was used for stimulus presentation, calibration of instruments, and data analysis. It can be found at:
http://www.mathworks.com/products/matlab/

Python Software: This software was used for data analysis. It can be found at:
https://www.python.org/

Mathematica Software: This software was used for behavioral and data analysis. It can be found at:
https://www.wolfram.com/mathematica/

RELACS Software: This software was used for acoustic emission recording and analysis. It was first used in (Benda et al., 2007) can be found at:
https://sourceforge.net/projects/relacs/

3.7 CODES

boxStimuli: This code took into account the timing of the control and stimulus presentations, as well as the mouse's position during the trial by maintaining a datalink with the inline camera through a User Datagram Protocol (UDP). This code was used in 'The Box' paradigm.

movementAnalysis: This code extracted positional data in relation to 'The Box' paradigm. Incorporated within this code was the implementation of a median filter

over a 20 millisecond period in order to minimize the noise which the mouse tracking software BioBServe measured due to the small shifts in centroid position of the mouse as a result of the imperfect representation of the mouse by the software.

stripeAdjust: This code ensures that the visual resolution set by the experimenter is maintained throughout stimulus presentation despite movement of the mouse. Conceptually, the code is visualized in figure 10. In words, a virtual striped cylinder, centered on the mouse's head, was projected onto the monitors. In practice, this would require the stripes to expand when the distance increases and vice versa. This code was used in the Optokinetic Reflex Drum paradigm, and first described in (Benkner et al., 2013).

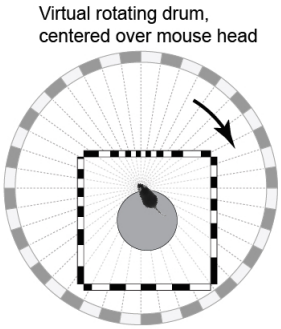

Figure 10: Visual conception of stripeAdjust code. Taken from (Benkner et al., 2013)

loomingBehaviorUniqueness: This code performed the calculations to establish the Behavioral Uniqueness of reactions to the Looming Stimulus paradigm.

4

RESULTS

The results of this study will be broken into two main sections: first, the results from the three groups of Albino mice (wild type, rd1, and rd1 with ChR2 expression); and second, the results from the two groups of the Bern mice (rd1, and rd1 with Opto-mGluR6 expression). All groups underwent behavioral testing within 'The Box' paradigm. Only the Bern groups completed behavioral testing in the Optokinetic Reflex Drum and the Looming Stimulus paradigms, as the Albino WT mice showed no behavioral responses to these stimuli in pilot experiments.

4.1 RESULTS: ALBINO GROUPS

The main paradigm with which visual abilities were measured within the Albino groups was 'The Box'. This paradigm allowed stimulus presentation on computer monitors while position and movement data from each mouse was extracted. Several different experimental trials were conducted in which stimuli were presented for 1-minute time, including: a full field stimulus, where both computer monitors changed from black to white; a 4Hz flicker stimulus, where one monitor flickered at 4Hz with 100% contrast while the other monitor maintained a neutral gray; a 10Hz flicker stimulus, where one monitor flickered at 10Hz with 100% contrast while the other monitor maintained a neutral gray; and moving stripes, where both monitors displayed a black and white cyclic pattern of stripes which drifted at 0.5 or 1.2 cycles per second and had a width of 5.4cm per cycle. Additionally, 'The Box' allowed for measurements of avoidance and preference behavior through the Light / Dark Box paradigm, where after some time, one monitor was set to black and one monitor was set to white and the duration spent on each side was measured. This was expanded in the Bern groups with an extra trial measuring avoidance behavior in the context of a 4Hz flicker.

Significant findings were seen in the Albino WT group during the full field, 4Hz flicker, and 10Hz flicker trials. No significant findings were seen in any of the conditions within the Albino groups having retinal degeneration, regardless of ChR2 expression. Futhermore, in the Light / Dark Box paradigm, it does appear there is a trend toward preference for the dark within the WT group, with 4 out of 6 mice showing strong preference for such. However, with small group size and without unanimity, this result is only suggestive and was not found to be significant. Lastly, analysis of behavioral reactions to the looming stimulus in pilot studies showed no noticeable reactions whatsoever to the stimulus. The Albino mice did not perform the Optokinetic Reflex Drum tests because albino mice in general are known not to display such a reflex.

Within context of "The Box", figure 11 represents significance measures of all previously mentioned experimental trials across all groups.

			Groups		
	Albino WT	Albino rd1	Albino ChR2	Bern Opto-mGluR6	Bern rd1
Full Field	+	not significant	not significant	not significant	not significant
Full Field (repeat)	+	not tested	not tested	not tested	not tested
4Hz Flicker	+	not significant	not significant	-	+
4Hz Flicker (repeat)	+	not tested	not tested	not tested	not tested
10Hz Flicker	+	not significant	not significant	not tested	not tested
10Hz Flicker (repeat)	not significant	not tested	not tested	not tested	not tested
Moving Stripes (0.5cps)	not significant	not tested	not tested	not tested	not tested
Moving Stripes (1.2cps)	not significant	not significant	not significant	not significant	not significant
Moving Stripes (1.2cps, repeat)	not significant	not tested	not tested	not significant	not significant
Light Dark Box	not significant	not significant	not significant	not significant	not significant
Flicker Avoidance	not tested	not tested	not tested	not significant	not significant

Figure 11: +/- indicates a significant increase or a decrease in movement behavior during the stimulus period relative to the control period.

Furthermore, analysis between the minute of control leading up to the one minute of stimulus for the Albino WT mice can be seen in figure 12 and figure 13. The analysis within this paradigm took the total movement of each mouse during this entire 2-minute testing period and then normalized the movement from the control and stimulus periods into a percentage.

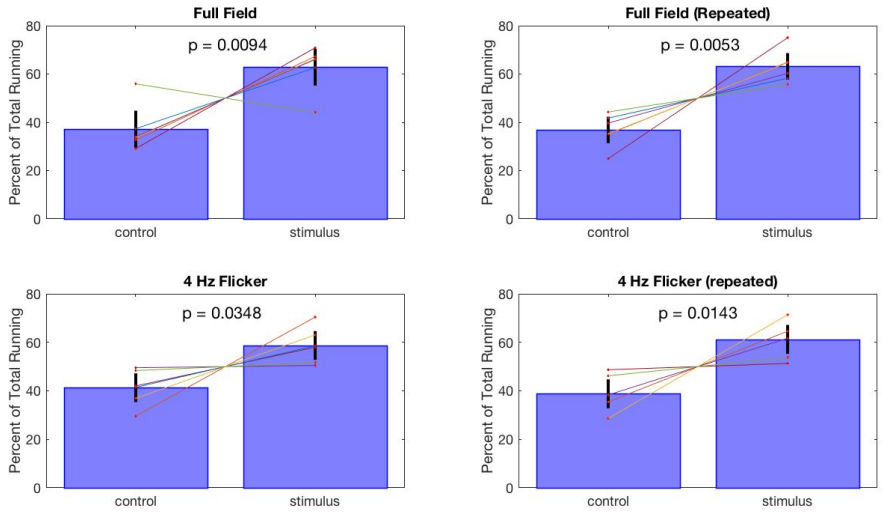

Figure 12: Albino WT: Continued Experiments. Total distance covered in 60 seconds of control versus 60 seconds of stimulus. Lines represent individual mice.

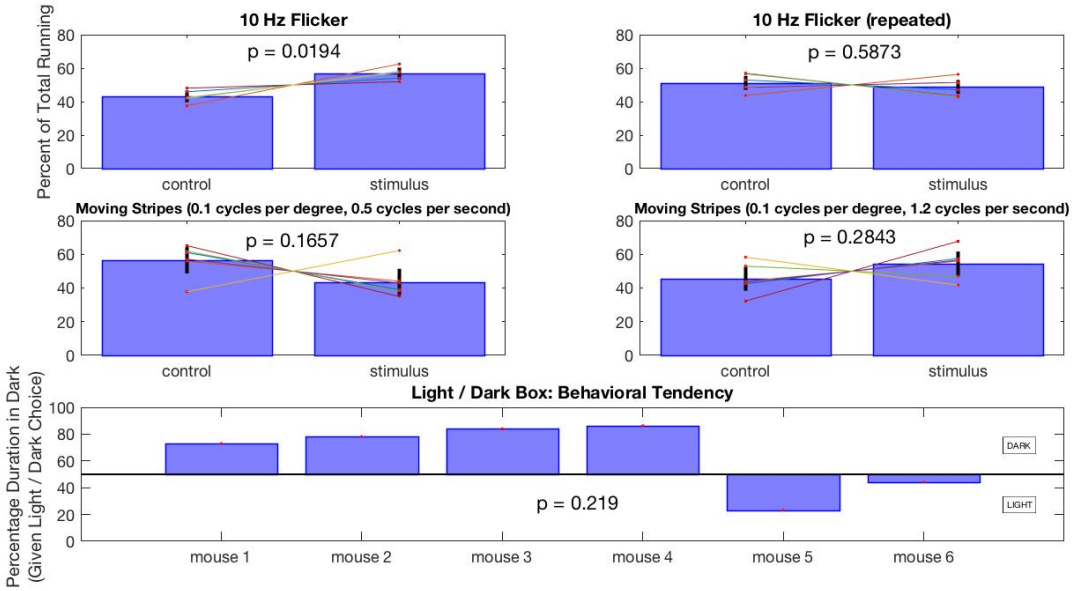

Figure 13: Albino WT: Total distance covered in 60 seconds of control versus 60 seconds of stimulus. Lines represent individual mice. Additionally, the bottom graphic shows percentage of time spent in the dark over 2 minutes time.

The results gathered across all trials within 'The Box' for the Albino ChR2 (figure 14) and Albino Rd1 (figure 15) groups showed no significance with regard to measured distance moved during the stimulus vs. the control periods. The Light / Dark Box results also do not show any trends toward preference to one condition over the other.

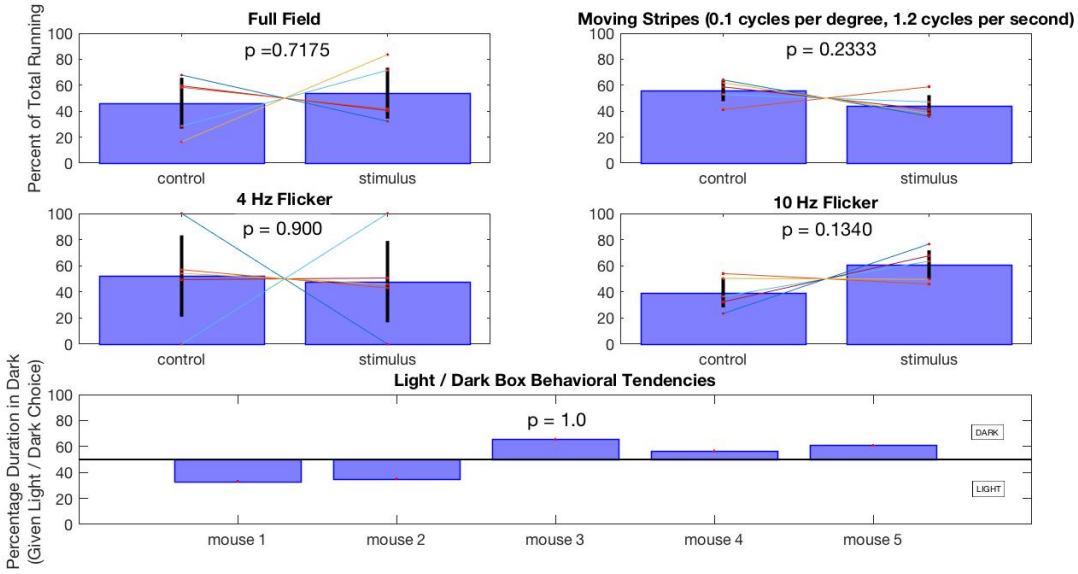

Figure 14: Albino ChR2: Total distance covered in 60 seconds of control versus 60 seconds of stimulus. Lines represent individual mice.

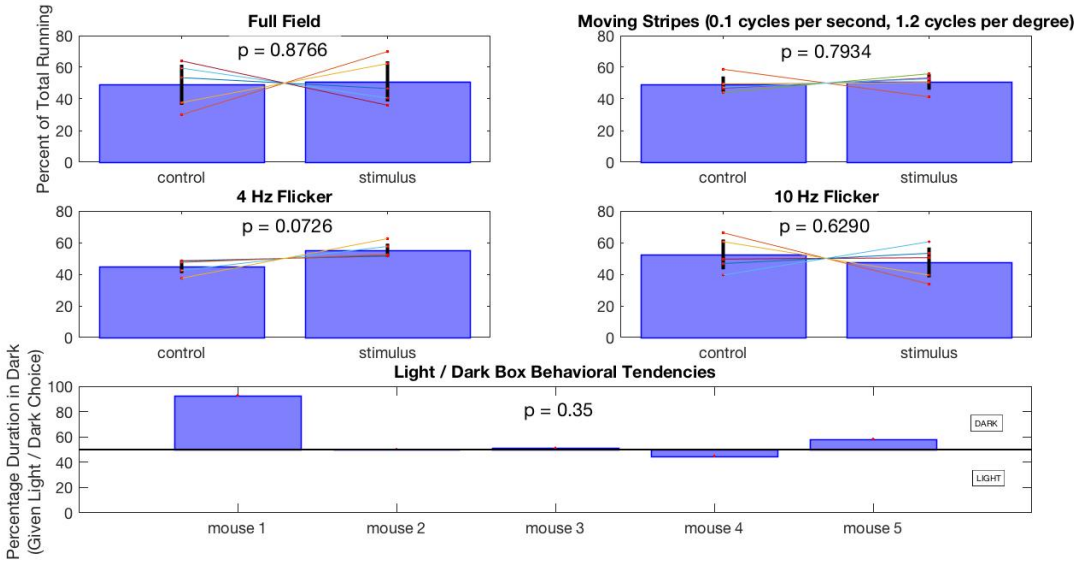

Figure 15: Albino Rd1: Total distance covered in 60 seconds of control versus 60 seconds of stimulus. Lines represent individual mice.

4.2 RESULTS: BERN GROUPS

The paradigms used with the Bern mice groups were much more expansive and included the Optokinetic Reflex Drum to assess visual acuity in relation to contrast, and the Looming Stimulus paradigm, which measured instances of unique behavioral responses to a potentially threatening stimulus. Within "The Box" paradigm, the following experimental trials were presented: a full field stimulus, where in difference to the Albino groups, only one computer monitor changed from black to white; a 4Hz flicker stimulus, where one monitor flickered at 4Hz at 100% contrast while the other monitor maintained a neutral gray; moving stripes, where both monitors displayed a black and white pattern of stripes which drifted at 1.2 cycles per second and were 5.4cm per cycle in width; and the Light / Dark Box, where one monitor displayed full contrast black, and the other displayed full contrast white.

Visually guided behavior was seen in "The Box" paradigm for the 4Hz flicker condition in both the Bern Opto-mGluR6 and the Bern Rd1 groups. However, in the treated group this behavior was seen as a decrease in the movement in 6 out of 7 mice at $p = 0.0236$, while in the untreated group this behavior was seen as an increase in movement in 4 out of 4 mice at $p = 0.0054$. This represents a significant difference between groups at $p = 0.0042$ according to a Student's two-tailed unpaired t-test. No other conditions suggested that either group responded with visually guided behavior to the stimulus. Furthermore, while the Looming Stimulus elicited responses, it did so in both groups, as can be seen in figure 16.

		Behaviorally Unique Response to Looming Stimuli				
		BoG (P225)	BoG (P235)	BoG (P275)	WoG (P230)	WoDG (P270)
Treated Mice						
Bern Opto-mGluR6						
	Mouse 1	yes	no	yes	no	yes
	Mouse 2	yes	yes	no	no	yes
	Mouse 3	yes	no	no	no	yes
	Mouse 6	maybe	no	no	no	yes
	Mouse 7	yes	maybe	yes	no	maybe
	Mouse 9	yes	yes	yes	no	yes
	Mouse 10	yes	no	no	no	yes
Untreated Mice						
Bern rd1						
	Mouse 4	yes	yes	no	no	yes
	Mouse 5	no	yes	no	no	no
	Mouse 8	yes	no	yes	no	no
	Mouse 11	yes	yes	no	maybe	yes

Figure 16: Bern Groups: Categorization of behaviorally unique responses to the Looming Stimulus at different ages and stimuli. BoG = Black disc on Grey, WoG = White disc on Grey, WoDG = White disc on Dark Gray.

In the treated group, within the repeated stimulus condition of a black disc on a gray background, 86%, 14%, and 43% of mice responded with behavior that suggested that they have seen the stimulus. This conclusion was based on the frequency at which different behaviors occurred, supported by visual observance and confirmation of the mouse's reactive behavior. When looking at the untreated group a similar pattern emerges, where 75%, 75%, and 25% mice responded with behavior that suggested that they saw these stimulus presentations. Both groups displayed more reactions to the white on dark gray stimulus at P270 than the last black on gray stimulus at P275. While neither group responded to the white on gray stimulus at P230.

Analysis of the results gathered from the Optokinetic Reflex Drum show better contrast thresholds at all tested spatial resolution levels within the treated group, as can be seen in figure 17. Furthermore, contrast sensitivity appears to decrease as a group through time in the untreated but not in the treated group.

	Contrast Sensitivity														
Experimental Day			P232					P272					P307		
Treated Mice															
Bern Opto-mGluR6	0.05	0.06	0.15	0.35	cpd	0.05	0.06	0.15	0.35	cpd	0.05	0.06	0.15	0.35	cpd
Mouse 1	100	50		N/A		N/A	50	75	75		N/A	25	25		
Mouse 2		100	100	N/A		N/A	25	25			N/A	50	15		
Mouse 3	50	20	50	N/A		N/A	10	15	75		N/A	50	100	100	
Mouse 6	75	75	100	N/A		N/A	75				N/A	100	50		
Mouse 7	10	20	100	N/A		N/A	100	50			N/A	50	75		
Mouse 9	50	20	50	N/A		N/A	50	75			N/A	15	10		
Mouse 10	75	75		N/A		N/A	50	25	75		N/A	25	75		
Untreated Mice															
Bern rd1	0.05	0.06	0.15	0.35		0.05	0.06	0.15	0.35		0.05	0.06	0.15	0.35	
Mouse 4	100	75		N/A		N/A	75	75			N/A	50	100		
Mouse 5	75	100		N/A		N/A	75				N/A				
Mouse 8	10	7	7	N/A		N/A	100		100		N/A				
Mouse 11	75	75	100	N/A		N/A	75				N/A		100	100	
		= no response													

Figure 17: Bern Groups: Contrast Thresholds (in Michelson contrast values) across different spatial resolution levels. N/A represents not-tested paradigm/group combinations.

Expanding upon this, two main components from these results can be examined: first, the stability of contrast sensitivity across time; and secondly, the threshold of such contrast sensitivity in context of different spatial resolutions and ages. In the treated group, in the 40 days between P232 and P272, reductions in contrast sensitivity were seen in 29% of mice in the 0.06 cycles per degree (cpd) condition, and only 14% of mice in the 0.15 cycles per degree condition. The results from the untreated group over the same time show reductions of contrast sensitivity within 25% of mice in the 0.06 cpd condition, and 67% of mice in the 0.15 cpd condition. These differences are also seen in the 35 days between P272 and P307. Here, although 43% of treated mice show reductions in both the 0.06 cpd and 0.15 cpd conditions, 75% of untreated mice showed a reduction to the 0.06 cpd condition and 100% of untreated mice showed a reduction to the 0.15 cpd condition.

We can see that the treated mice have more sensitive contrast thresholds when comparing overall group results at different spatial resolutions, especially at P272 and P307. This group difference in contrast sensitivity is seen clearly when examining detections at or below 50% contrast. Across these two experimental dates, only a single mouse in the untreated group displayed a visually guided behavior to this contrast level within the 0.06 cpd condition, and no mice in the untreated group displayed such behavior in the 0.15 cpd condition. In the treated group, 6 out of 7 mice met this criteria in the 0.06 cpd condition, and 5 out of 7 mice met this criteria at the 0.15 cpd condition. The one condition that neither group performed well in was the spatial resolution of 0.35 cpd, with only a single mouse from each group detecting the stimulus at P307. When looking at general response behavior through time to the spatial resolution of 0.15 cpd, 86% of the treated group had positive responses at P272, compared to 25% of the untreated group. At P307, 100% of the treated group showed responses, while 50% of the untreated group showed responses. These basic response differences through time are further illuminated when examining the largest repeated condition of 0.06 cpd. Here, both groups displayed a 100% detection rate to the stimulus at 100% contrast at P272, but while the treated group maintained this 100% group response at P307, the untreated group fell to a 25% detection rate.

Results from 'The Box' for the Bern Opto-mGluR6 group can be seen in figure 18. Visually guided behavior was found only in the 4Hz flicker condition.

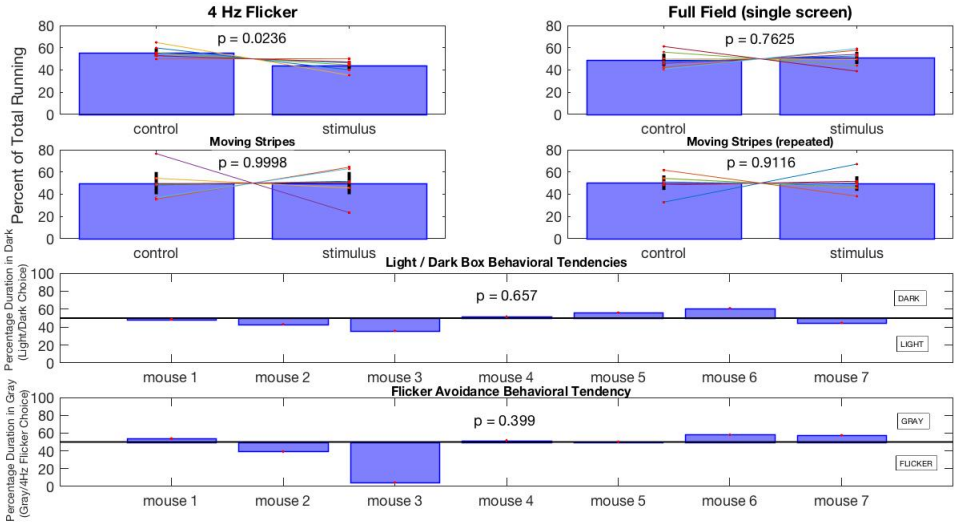

Figure 18: Bern Opto-mGluR6: Total distance covered in 60 seconds of control versus 60 seconds of stimulus. Lines represent individual mice.

Results from 'The Box' for the Bern Rd1 group can be seen in figure 19. Visually guided behavior was found only in the 4Hz flicker condition.

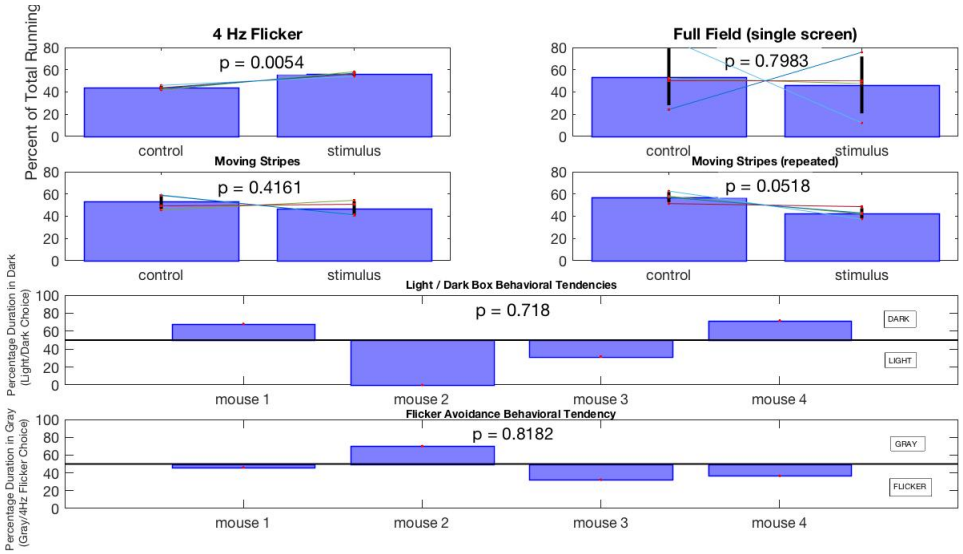

Figure 19: Bern Rd1: Total distance covered in 60 seconds of control versus 60 seconds of stimulus. Lines represent individual mice.

Figure 20 represents the results of the Optokinetic Reflex Drum graphically. It is here apparent that at P307 the Opto-mGluR6 treated group is able to successfully detect spatial resolutions at much lower contrasts than the untreated group.

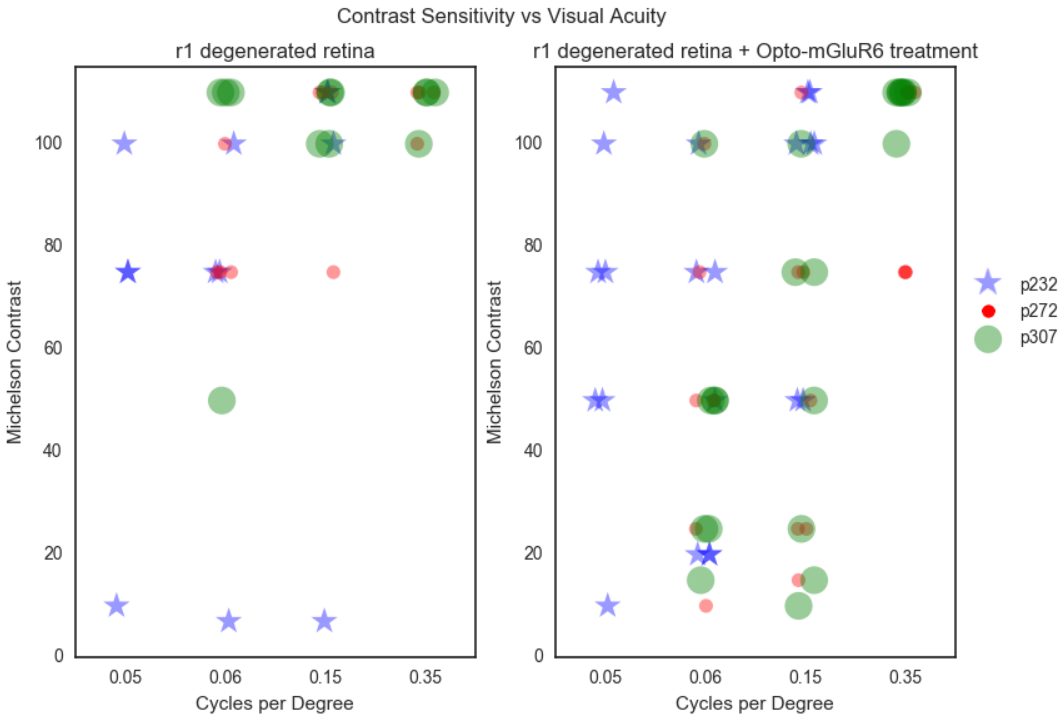

Figure 20: Bern Groups: Reached Contrast Thresholds for varying spatial resolutions across different ages. Each data point represents the best performance from an individual mouse within the respected group at a certain age. Data points above 100 Michelson Contrast represent a failure altogether to detect the stimulus.

Lastly, figure 21 shows graphically the behavioral uniqueness values in histogram format from the "Looming Stimulus" as represented through time, conditions, and ages. The higher values on the y-axis represent instances of higher behavioral uniqueness, in general, these unique behaviors occur during the stimulus presentations.

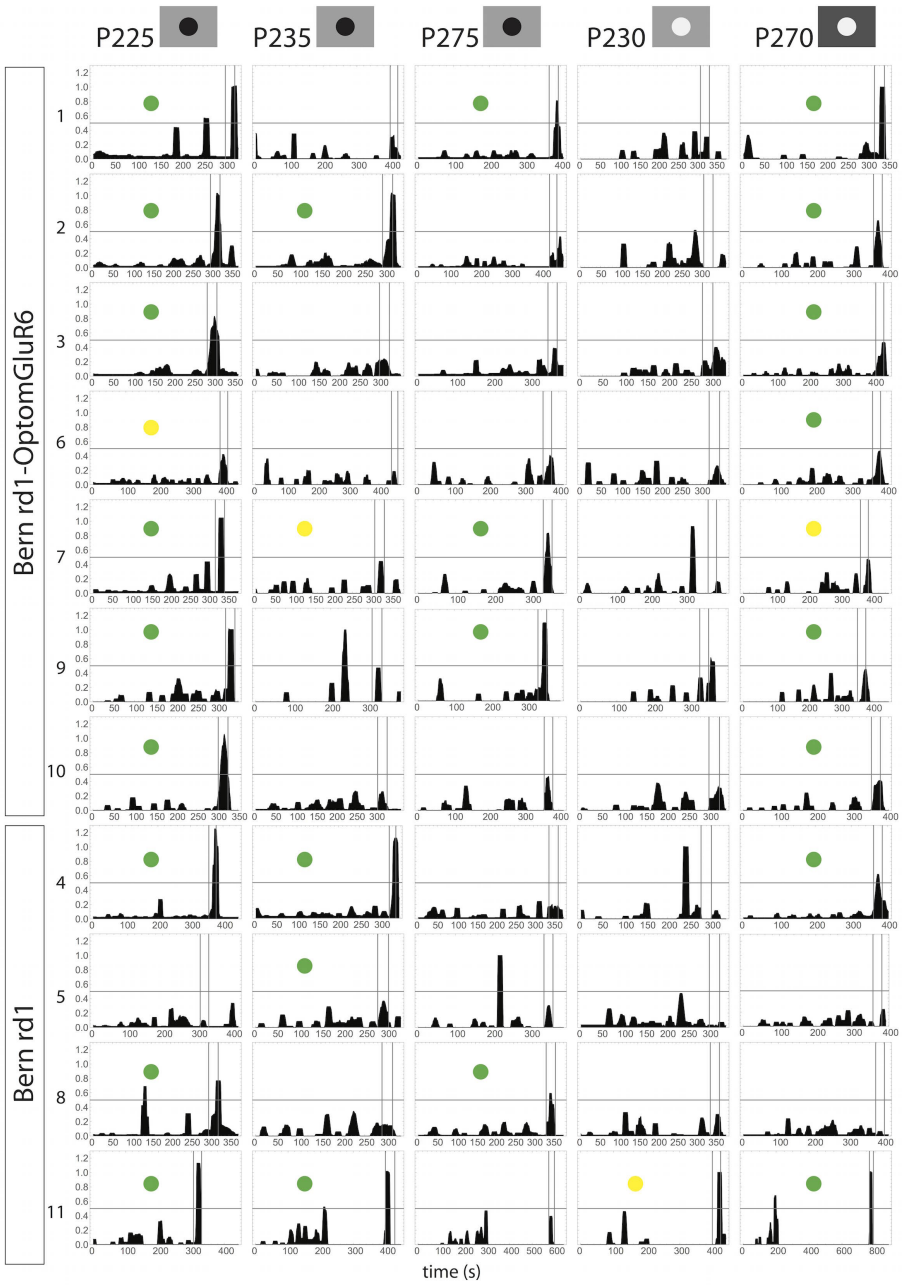

Figure 21: Bern Groups: Vertical lines display stimulus period. Green dots represent behavioral uniqueness during stimulus, while yellow represent possible behavioral uniqueness. The x-axis represents time, and the y-axis represents the behavioral uniqueness value, see methods section for explanation.

5

DISCUSSION

The goal of this project was to determine the extent to which optogenetic treatments could restore vision in a degenerating retina. In order to accomplish this aim, different behavioral paradigms were created in attempt to tease apart the visual abilities from mice who have had and have not had these optogenetic treatments. Upon examination of the results, two trends appear: first, the mice who have had ChR2 expressed in the ON-bipolar cells, as well as their Rd1 counterparts, seem to be unresponsive to any behavioral stimuli; second, the mice who have had Opto-mGluR6 expressed in the ON-bipolar cells, as well as their Rd1 counterparts, seem to be responsive to many of the behavioral stimuli, which is partly in line with the findings reported by (Wyk et al., 2015). The referenced study shows that activity within V1 is present in both groups at P180, but stimulus-driven V1 activation responses approach zero within the Rd1 group at P282. Yet, when visual responses are examined in the behavioral realm, it can be seen that the border between the treated and untreated group is not so clear cut; as both groups show evidence of ecological vision even as late as P307, the last experimental date.

Addressing the Albino mice first, the most likely situation is that the light levels emitted by the computer monitors (maximum production of 1100 lux given full intensity white at 5cm distance) do not produce the necessary light levels for stimulation of ChR2 (10^{15} photons $s^{-}1cm^{-}2$ as reported in Lagali et al., 2008). Due to this, despite whether or not the mice have the ChR2 treatment, the visual environment will be the same for all Albino groups with rd1 expression. Since these groups are then effectively the same, the behavioral measures would then be uninformative with respect to the questioned benefit of ChR2 expression. Therefore differences across the Albino groups of mice will no longer be discussed as no further insights can be gathered from their behavioral results

When looking at the Bern mice in context of Opto-mGluR6, three questions arise:
1) Did the Opto-mGluR6 treatment increase functional visual abilities?
2) Could the Opto-mGluR6 treatment have acted as a confusing and non-productive addition to visual perception?
3) Does Opto-mGluR6 serve as something that can delay retinal degeneration?

The main question can be examined in context of comparing behavioral results from different time points between the treated and untreated Bern mice groups. Results coming from the paradigms of "The Box" and the "Looming Stimulus" do not show convincing group differences, however the results from the "Optokinetic Reflex Drum" do suggest that Opto-mGluR6 may improve visual abilities in comparison with their rd1 counterparts.

Within "The Box", only the 4Hz flicker stimulus resulted in a visually guided behavior. However, both groups responded to this stimulus, and they did so in opposing ways, as seen in figure 18 and 19. The diverging results are interesting and result in a significance difference between groups at $p = 0.0042$, yet this finding is curious and asks whether this difference can be attributed to a real biological phenomena or whether it is a result of chance. Significance testing inherently gives false positives, compounding this is the fact that multiple tests were ran within this paradigm. Additionally, this finding was examined in more detail by comparing only the 30 seconds before and during stimulus presentation, and in this case, the significance disappeared. To account for the change in the "control" portion of the comparison, bootstrapping was done in which many 30 random 1-second segments were taken from portions of the total control behavior and each was compared to the 30 seconds of stimulus behavior. The significance was still not present. Since significance is seen in the same test when the analysis is extended to 60 seconds before and during the stimulus, this means that either the flicker causes behavior which is more profound in the latter 30 second period of the stimulus, or that the finding is by chance. With that being said, the untreated group showed similar behavior tendencies as the Albino WT mice, who displayed increases in movement behavior in two separate trials of the 4 Hz stimulus (figure 12). However, for opposing biological responses to the same visual stimuli to occur, there would have to be a plausible mechanism through which this occurs. The greatest potential for this is the Opto-mGluR6 mechanism itself, which has been shown to produce an inversed polarity in bipolar cells in response to light, so perhaps this flicker activates a different set of visual circuitry within the treated mice when compared to their untreated counterparts, which then either drives or inhibits locomotion. The results gathered from "The Box" can also be compared to the findings from Cehajic et al. (Cehajic-Kapetanovic et al., 2015), who treated mice with an ectopic expression of human rod opsin. Their results also showed this opposing group effect to the 4Hz flicker, seen as a decrease in visually driven movement in the treated group and an increase in visually driven movement in the wild-type group. The decrease in locomotor activity of their treated group is in line with the results from the treated group examined here, whereas the results from the wild-type are in line with the results from the untreated group examined here. It can be rationalized that both treated groups would show similar locomotive behavior due to similar

visual abilities, but one wonders why the WT and rd1 groups should also show similar locomotive behavior given that their visual abilities are certainly differing. Yet, the same study also found significant differences in visually driven behavior across a range of spatial resolutions within the moving stripes condition which were not found in the current study. Additionally, preference or avoidance behavior in both the light / dark box paradigm and to the flicker does not seem to be present in any of the 5 tested groups, diverging from previous results which find clear preference for the dark zone in wild-type mice (Bourin and Hascoët, 2003), (Takao and Miyakawa, 2006). Taken altogether, the lack of differentiating results from "The Box" suggest that either the analysis method or the paradigm is not fit for such fine-tuned group discriminations, or that behavioral reactions to the stimuli do not exist, or if they do exist, the displayed behavior is not different between the Opto-mGluR6 and rd1 groups. In any case, and importantly, these findings suggest that the untreated group displayed a visually guided behavior through a reaction to the stimulus. This indicates that the rd1 group may also have residual visual abilities around this time (P230), which is further supported by the results from the Optokinetic Reflex Drum and the Looming Stimulus.

When looking at the next paradigm, the Looming Stimulus, it can be seen that behavioral reactions exist through all time points of repeated testing with the black looming disc (P225, P235, P275). However, since these behavioral reactions exist in both groups, it suggests that this stimulus elicits such strong responses that any residual vision may lead to its detection. The decrease in responsiveness between the first and second presentations can be thought to be attributed to habituation effects as described in (Yilmaz and Meister, 2013), whereas the difference between the first and third presentation may be partly due to these same habitation effects, as well as potential degeneration in the retina. However, behavior in response to the white disc on dark gray background stimulus at P270, in which 86% treated mice showed unique behavior, would serve to attribute this decrease from the initial behavioral reactions to habituation to the same stimulus rather than to retinal degeneration. The untreated group also showed a stronger response to the P270 white disc on dark gray background stimulus than to the P275 black disc. Interestingly, no mice from either group responded to the white disc on gray background stimulus at P230, suggesting that either the lowered contrast compared to the dark gray background (Michelson contrast 50% vs 85%) prevented a behavioral response, or that there were again habituation effects from the initial trial at P225. Evidence from the Optokinetic Reflex Drum taken from around the same time (P232) shows that 57% of mice in the treated group and 25% of mice in the untreated group responded to the stimulus given a 50% contrast, suggesting that the gray background should be possible to detect for at least some mice. Taking all trials together, both groups showed behavioral responses rather equally with only 1 mouse from each

group not displaying noticeably unique behavior at first exposure (see figure 16). Therefore, for any differences to be seen, if there are any, larger and equal group sizes may be needed. It may also be the case that this stimulus invokes activity in such powerful evolutionary based circuits that any visual resources available contribute to the stimulus' detection. If this is true, it would suggest on one hand that the Looming Stimulus is not sensitive enough to discriminate between different levels of visual abilities, while on the other hand support its use in experimental paradigms where behavioral evidence of complete retinal degeneration was necessary. In any case, like "The Box", it appears that the results gathered from the Looming Stimulus do not tend to suggest anything about the effect of Opto-mGluR6 on functional vision due to the general inability to discriminate between the behaviors of the untreated and treated groups within the paradigm tasks.

Before going into the results of the Optokinetic Reflex Drum, we must first discuss the issue of "false positives" within this paradigm in particular. There are two types of false positives that can occur in this setup, those that are generated through an error in the detection algorithm, and those that are generated through congruent but random biological motion. The first type happens at a rate of around 1.9% as described in (Benkner et al., 2013), and can be virtually eliminated by concurrent manual observation. I manually checked every positive detection by the algorithm, thereby eliminating this type of false positive result. However, the second type of false positive, those caused by congruent biological movement, are currently unavoidable. It is simply not currently possible to determine whether the mouse was following the stimulus movement due to an actual perception of it, or whether it was simply producing this head movement by chance. Ideally, if one could sample enough behavior, one could develop a characteristic movement profile that the algorithm may be able to take into account to assist with this issue.

With that being said, the Optokinetic Reflex Drum paradigm was sensitive enough to elucidate different levels of visual abilities, and therefore distinguish between the treated and untreated groups. Referring back to figures 17 and 20, one can see a sharp loss of contrast sensitivity within the untreated group between P232 and P272. This loss of contrast sensitivity is taken even further by P307. It can be thought that retinal degeneration has more fully taken place around this age and the decline of contrast sensitivity can be expected. Interestingly, it appears that the contrast sensitivities of the treated group remain mostly constant, and they even improve in some circumstances. These individual improvements could be the result of several things: first, it could be due to false positives, but this then should also be seen in the untreated group; second, it could be due to familiarization and comfort with the paradigm; or third, it could be due to a more complete utilization of Opto-mGluR6 in light of a more fully degenerated photoreceptor layer. On this

latter point, if retinal input were coming from both remnant photoreceptors and the Opto-mGluR6 ON-bipolar cell mechanism, there could be contradictory and confusing input to the visual system. This double-input would in theory reduce as retinal degeneration progressed and photoreceptors died, potentially giving way to more coherent visual environments sensed primarily through Opto-mGluR6.

These interpretations, taken in combination with the group differences in contrast sensitivity seen in the Optokinetic Reflex Drum at P272 and P307, clearly draw a line between the visual abilities of the two groups. This difference may support the idea that mice lose some aspect of contrast sensitivity and acuity vision in this retinal degeneration model, which is then provided through expression of Opto-mGluR6.

Whether or not the Opto-mGluR6 treatment could pose confusing and non-productive additions to visual perception can be assessed by looking at the prior behavioral analysis between groups. The question itself is grounded in subjective experience with vision restoration methodologies primarily by patients of sub-retinal implants, who report experiences where the visual input was disturbing or unproductive (Yanai et al., 2007). Yet, as in no circumstance mice from the treated group displayed visual behavior inferior to the untreated group, it can be said that at least in the context of these experiments and in these mice, Opto-mGluR6 does not pose as a threat to the reduction of visual ability. Furthermore, as previously mentioned, increased contrast sensitivity in some mice was also seen later in life. Though, this effect is seen less in the untreated group, suggesting that perhaps these improvements in contrast sensitivity by the treated group could be due to a more complete 'take over' of visual duties by the Opto-mGluR6 mechanism as a result of the progressive degeneration of the retina, potentially eliminating a counter-productive double-input coming from both the optogenetic protein and any surviving photoreceptors which would have been more thoroughly present in the earlier stages of retinal degeneration. Whether or not this applies in humans, or that the subjective experience of the visual perceptions afforded by the addition of Opto-mGluR6 can be regarded negatively remains to be seen and is far outside the reach of the findings gathered in this thesis.

The question regarding Opto-mGluR6 serving as something to delay retinal degeneration cannot be analyzed with the current experimental paradigm, as the physical and exact level of degeneration cannot be assessed with only behavioral results. In order to answer this question, histological and electrophysiological methods should be applied, and a time line is in place for this to begin in December 2016.

Taking these findings in mind, there is an obvious experimental disadvantage to the presence of visually guided behavior in the untreated retinal degeneration group. These disadvantages manifest because if the degeneration is not complete, visual abilities are subject to variance between individual mice, and furthermore, individual mice may respond different to the same incomplete visual signals, making group comparisons more difficult to analyze. Yet, as this visually guided behavior is present in some of the rd1 mice even surprisingly late in life (P307), the rate of degeneration can be thought to best mimic the slow and incomplete retinal degeneration that a human may suffer from. Additionally, the treatment in context of this slower degeneration would best mimic the potential treatment option in a clinical setting. It is possible that if experiments were conducted at an even later date, retinal degeneration would have more completely removed all visual responses and left only the Opto-mGluR6 mechanism to conduct any visual input, as may be the case between P272 and P307. This will be further tested in December 2016, along with the planned histological and electrophysiological methods. It is also possible that retinal degeneration had taken place, and light responses could be attributed to the Melanopsin RGC, as they are sensitive in roughly the same spectral range as the M-cone. However, these cells have 15 degree visual angles, are extremely sustained, and have poor spatial resolution, all of which lead to the thought that although they may be able to detect an environmental stimulus such as a full field change in illumination, they would not be responsible for something such as the visual acuity needed in the Optokinetic Reflex Drum (Münch, Euler, and Baden, 2015).

5.1 IMPROVEMENTS AND CONSIDERATIONS

To better understand the mechanisms at work, it would be wise in future experiments to also examine the electrical activity in the visual circuitry through electrophysiology, as well as determine the degeneration of the retina and expression of Opto-mGluR6 within the bipolar cells and their connections to RGCs through histological methods, as planned. By coupling these findings with the behavioral results, the role and integration of the optogenetic protein can be better understood. Another consideration would be to ensure that all tested mice groups can perform all tasks, unlike mice with an albino background, which genetically lack the optokinetic reflex. This was particularly inopportune, as the Optokinetic Reflex Drum proved to be one of the most sensitive behavioral measures, and the absence of comparison across optogenetic proteins in this task leaves room for improvement. Furthermore, for comparative measures, it would be essential to acquire wild-type, optogenetically treated, and rd1 littermates for each mouse strain. The Bern mice were separated only into rd1 and rd1/Opto-mGluR6 groups. As the reasons behind behavioral responses to tasks can only be hypothesized given

the experimental nature of the study, having the wild-type "normal" response of this mouse strain would have been advantageous for comparison purposes. Larger group sizes would also increase statistical power and therefore allow the behavioral paradigms to become more sensitive. The uneven group sizes of the Bern mice (7 treated and 4 untreated) was also not ideal. Furthermore, there is reason to believe that something such as Environmental Enrichment (EE) could be responsible for the delayed degeneration of these particular mice. Prior studies have shown increases of up to 18% in visual acuity and prolonged photoreceptor life from rearing in environments containing even something as simple as a wooden tunnel within the cage, such as was used within the current study (Barone et al., 2012). To examine this effect more in detail, it would be necessary to separate the groups into mice who underwent behavioral testing and mice that did not. As surely the changing environments and handling of the mice contributed to the diversity which underlies the concept of EE. Then, at a later date, a final behavioral measure along with electrophysiological and histological methods could be conducted to determine if the degeneration was delayed in the group whose environment was most changing and rich. Conversely, the mice were housed in cages which were exposed to light levels in the housing room of around 500 lux at 2 meter distance. This is much brighter than the experimental room (175 lux at 2 meter distance), and even the highest intensity gathered from the neutral gray setting of the monitors (330 lux at 5cm distance). Since the normal housing environment produced conditions which were brighter than some of the monitors within behavioral trials, potential habituation effects could have occurred and influenced experimental results. Additionally, this home environment could have also posed damaging effects to the photoreceptor layer, as reduced light exposure has been suggested as an ameliorative therapy for hereditary photoreceptor degeneration in humans (Liu et al., 2009). In future studies, light environments should be chosen carefully and intentionally based on literature to suit the questions of the study.

5.2 CONCLUSION

In conclusion, in its current state, ChR2 expression requires levels of light intensity which are both toxic and not fit for use in clinical settings hoping to restore everyday visually guided behavior (Wyk et al., 2015), (Hunter et al., 2012). On the other hand, results from the Optokinetic Reflex Drum suggest that Opto-mGluR6 may be an optogenetic protein that grants stable improvements in visual abilities, such as contrast sensitivity and visual acuity. However, conducting experiments later in the time line of retinal degeneration, larger and complete groups, more sensitive paradigms, intensive familiarization with these paradigms, and data coupling with electrophysiological and histological methods is necessary to more completely see the impact of Opto-mGluR6 on vision restoration.

BIBLIOGRAPHY

Antkowiak, Bernd (2015). *Neurophysiology*. University of Tübingen Lecture.

Bainbridge, James WB et al. (2008). "Effect of gene therapy on visual function in Leber's congenital amaurosis." In: *New England Journal of Medicine* 358.21, pp. 2231–2239.

Barone, Ilaria et al. (2012). "Environmental enrichment extends photoreceptor survival and visual function in a mouse model of retinitis pigmentosa." In: *PloS one* 7.11, e50726.

Beltran, William A (2008). "On the Role of CNTF as a Pontential Therapy for Retinal Degeneration: Dr. Jekyll or Mr. Hyde?" In: *Recent Advances in Retinal Degeneration*. Springer, pp. 45–51.

Benda, Jan et al. (2007). "From response to stimulus: adaptive sampling in sensory physiology." In: *Current opinion in neurobiology* 17.4, pp. 430–436.

Benkner, Boris et al. (2013). "Characterizing visual performance in mice: An objective and automated system based on the optokinetic reflex." In: *Behavioral neuroscience* 127.5, p. 788.

Bi, Anding et al. (2006). "Ectopic expression of a microbial-type rhodopsin restores visual responses in mice with photoreceptor degeneration." In: *Neuron* 50.1, pp. 23–33.

Bourin, Michel and Martine Hascoët (2003). "The mouse light/dark box test." In: *European journal of pharmacology* 463.1, pp. 55–65.

Busskamp, Volker et al. (2010). "Genetic reactivation of cone photoreceptors restores visual responses in retinitis pigmentosa." In: *science* 329.5990, pp. 413–417.

Busskamp, Volker et al. (2014). "miRNAs 182 and 183 are necessary to maintain adult cone photoreceptor outer segments and visual function." In: *Neuron* 83.3, pp. 586–600.

Cajal, Santiago Ramón y (1960). *Studies on vertebrate neurogenesis*. Charles C. Thomas Publisher.

Cajal, Santiago Ramón y (1972). *The structure of the retina*. Charles C. Thomas Publisher.

Cehajic-Kapetanovic, Jasmina et al. (2015). "Restoration of vision with ectopic expression of human rod opsin." In: *Current Biology* 25.16, pp. 2111–2122.

Chang, B et al. (2002). "Retinal degeneration mutants in the mouse." In: *Vision research* 42.4, pp. 517–525.

Doroudchi, M Mehdi et al. (2011). "Virally delivered channelrhodopsin-2 safely and effectively restores visual function in multiple mouse models of blindness." In: *Molecular Therapy* 19.7, pp. 1220–1229.

Douglas, RM et al. (2005). "Independent visual threshold measurements in the two eyes of freely moving rats and mice using a virtual-reality optokinetic system." In: *Visual neuroscience* 22.05, pp. 677–684.

Ebrey, Thomas and Yiannis Koutalos (2001). "Vertebrate Photoreceptors." In: *Progress in Retinal and Eye Research* 20.1, pp. 49 –94. ISSN: 1350-9462.

Einstein, Albert (1965). "Concerning an heuristic point of view toward the emission and transformation of light." In: *American Journal of Physics* 33.5, p. 367.

Felleman, Daniel J and David C Van Essen (1991). "Distributed hierarchical processing in the primate cerebral cortex." In: *Cerebral cortex* 1.1, pp. 1–47.

Fenno, Lief, Ofer Yizhar, and Karl Deisseroth (2011). "The development and application of optogenetics." In: *Neuroscience* 34.1, p. 389.

Feynman, Richard Phillips and A Zee (2006). *QED: The strange theory of light and matter*. Princeton University Press.

Fried, Shelley I, Thomas A Münch, and Frank S Werblin (2002). "Mechanisms and circuitry underlying directional selectivity in the retina." In: *Nature* 420.6914, pp. 411–414.

Hartong, Dyonne T, Eliot L Berson, and Thaddeus P Dryja (2006). "Retinitis pigmentosa." In: *The Lancet* 368.9549, pp. 1795–1809.

Hess, A and JZ Young (1952). "The nodes of Ranvier." In: *Proceedings of the Royal Society of London B: Biological Sciences* 140.900, pp. 301–320.

Hood, Donald C and Marcia A Finkelstein (1986). "Sensitivity to light." In: *Handbook of Perception and Human Performance (Vol. 1: Sensory Processes and Perception). John Wiley and Sons, New York.*

Hunter, Jennifer J et al. (2012). "The susceptibility of the retina to photochemical damage from visible light." In: *Progress in retinal and eye research* 31.1, pp. 28–42.

Huygens, Christiaan (2012). *Treatise on light*. tredition.

Jones, Howard, RE Latham, and Anthony M Esolen (1996). *Lucretius: On the Nature of the Universe*.

Kandel, Eric R et al. (2000). *Principles of neural science*. Vol. 4. McGraw-hill New York.

Keeler, Clyde (1966). "Retinal degeneration in the mouse is rodless retina." In: *Journal of Heredity* 57.2, pp. 47–50.

Kolb, Helga (2016). *Simple Anatomy of the Retina*. University of Utah Website.

Lagali, Pamela S et al. (2008). "Light-activated channels targeted to ON bipolar cells restore visual function in retinal degeneration." In: *Nature neuroscience* 11.6, pp. 667–675.

Lanyi, Janos K (1990). "Halorhodopsin, a light-driven electrogenic chloride-transport system." In: *Physiological reviews* 70.2, pp. 319–330.

Leskov, Ilya B et al. (2000). "The gain of rod phototransduction: reconciliation of biochemical and electrophysiological measurements." In: *Neuron* 27.3, pp. 525–537.

Li, Tianqing et al. (2013). "Multipotent stem cells isolated from the adult mouse retina are capable of producing functional photoreceptor cells." In: *Cell research* 23.6, pp. 788–802.

Lin, Bin, Richard H Masland, and Enrica Strettoi (2009). "Remodeling of cone photoreceptor cells after rod degeneration in rd mice." In: *Experimental eye research* 88.3, pp. 589–599.

Liu, Xiaoqing et al. (2009). "Increased light exposure alleviates one form of photoreceptor degeneration marked by elevated calcium in the dark." In: *PloS one* 4.12, e8438.

Mitchiner, James C, Lawrence H Pinto, and Joseph W Vanable (1976). "Visually evoked eye movements in the mouse (Mus musculus)." In: *Vision research* 16.10, 1169IN7–1171.

Münch, Thomas A (2013). "Visual behavior: mice run from overhead danger." In: *Current Biology* 23.20, R925–R927.

Mutter, Marion, Natalia Swietek, and Thomas A. Münch (2014). "Salvaging Ruins: Reverting Blind Retinas into Functional Visual Sensors." In: *Photoswitching Proteins*. Ed. by Sidney Cambridge. Vol. 1148. New York, NY: Springer New York, pp. 149–160. ISBN: 978-1-4939-0469-3 978-1-4939-0470-9.

Münch, Thomas, Thomas Euler, and Tom Baden (2015). *Retina as a Model Circuit*. University of Tübingen Lecture.

Nagel, Georg et al. (2002). "Channelrhodopsin-1: a light-gated proton channel in green algae." In: *Science* 296.5577, pp. 2395–2398.

Nagel, Georg et al. (2003). "Channelrhodopsin-2, a directly light-gated cation-selective membrane channel." In: *Proceedings of the National Academy of Sciences* 100.24, pp. 13940–13945.

Ölveczky, Bence P, Stephen A Baccus, and Markus Meister (2003). "Segregation of object and background motion in the retina." In: *Nature* 423.6938, pp. 401–408.

Pennesi, Mark E et al. (2012). "Long-Term Characterization of Retinal Degeneration in rd1 and rd10 Mice Using Spectral Domain Optical Coherence TomographySD-OCT Imaging of rd1 and rd10 Mice." In: *Investigative ophthalmology & visual science* 53.8, pp. 4644–4656.

Polosukhina, Aleksandra et al. (2012). "Photochemical restoration of visual responses in blind mice." In: *Neuron* 75.2, pp. 271–282.

Rasband, Matthew N and Elior Peles (2016). "The Nodes of Ranvier: Molecular Assembly and Maintenance." In: *Cold Spring Harbor perspectives in biology* 8.3, a020495.

Reinhard, Katja et al. (2015). "Retinal output changes qualitatively with every change in ambient illuminance." In: *Nature Neuroscience* 18.1.

Rizzo, Joseph F and John Wyatt (1997). "REVIEW: Prospects for a Visual Prosthesis." In: *The Neuroscientist* 3.4, pp. 251–262.

Rokem, Ariel (2007). *Visual Pathways*. University of California Berkeley Website.

Santos-Ferreira, Tiago et al. (2015). "Daylight vision repair by cell transplantation." In: *Stem Cells* 33.1, pp. 79–90.

Schaffel, Frank (2015). *Visual Systems*. University of Tübingen Lecture.

Smirnakis, Stelios M et al. (1997). "Adaptation of retinal processing to image contrast and spatial scale." In: *Nature* 386.6620, pp. 69–73.

Takao, Keizo and Tsuyoshi Miyakawa (2006). "Light/dark transition test for mice." In: *JoVE (Journal of Visualized Experiments)* 1, e104–e104.

Wallace, Damian J et al. (2013). "Rats maintain an overhead binocular field at the expense of constant fusion." In: *Nature* 498.7452, pp. 65–69.

Wässle, Heinz (2004). "Parallel processing in the mammalian retina." In: *Nature Reviews Neuroscience* 5.10, pp. 747–757.

Wong, Darren and Boo Hong Kwen (2005). "Shedding Light on the Nature of Science through a Historical Study of Light." In: *Redesigning Pedagogies: Research, Policy and Practice*.

Wyk, Michiel van et al. (2015). "Restoring the ON switch in blind retinas: opto-mGluR6, a next-generation, cell-tailored optogenetic tool." In: *PLoS Biol* 13.5, e1002143.

Yanai, Douglas et al. (2007). "Visual performance using a retinal prosthesis in three subjects with retinitis pigmentosa." In: *American journal of ophthalmology* 143.5, pp. 820–827.

Yilmaz, Melis and Markus Meister (2013). "Rapid innate defensive responses of mice to looming visual stimuli." In: *Current Biology* 23.20, pp. 2011–2015.

Young, Thomas (1801). "The Bakerian Lecture: on the mechanism of the eye." In: *Philosophical Transactions of the Royal Society of London* 91, pp. 23–88.

Zhang, Dao-Qi et al. (2008). "Intraretinal signaling by ganglion cell photoreceptors to dopaminergic amacrine neurons." In: *Proceedings of the National Academy of Sciences* 105.37, pp. 14181–14186.

Zrenner, Eberhart et al. (2011). "Subretinal electronic chips allow blind patients to read letters and combine them to words." In: *Proceedings of the Royal Society of London B: Biological Sciences* 278.1711, pp. 1489–1497.